ORNL/TM-6464

An Interim Analytical Description of the Creep and Creep-Rupture Behavior of ERNiCr-3 Weld Metal

M. K. Booker
R. L. Klueh

OAK RIDGE NATIONAL LABORATORY
OPERATED BY UNION CARBIDE CORPORATION · FOR THE DEPARTMENT OF ENERGY

Printed in the United States of America. Available from
the Department of Energy,
Technical Information Center
P.O. Box 62, Oak Ridge, Tennessee 37830
Price: Printed Copy $5.25; Microfiche $3.00

ORNL/TM-6464
Distribution
Category
UC-79b, -h, -k

Contract No. W-7405-eng-26

METALS AND CERAMICS DIVISION

AN INTERIM ANALYTICAL DESCRIPTION OF THE CREEP AND CREEP-RUPTURE BEHAVIOR OF ERNiCr-3 WELD METAL

M. K. Booker and R. L. Klueh

November, 1978

Prepared by the
OAK RIDGE NATIONAL LABORATORY
Oak Ridge, Tennessee 37830
operated by
UNION CARBIDE CORPORATION
for the
DEPARTMENT OF ENERGY

Blank Page

CONTENTS

AN INTERIM ANALYTICAL DESCRIPTION OF THE CREEP AND CREEP-RUPTURE BEHAVIOR OF ERNiCr-3 WELD METAL*

M. K. Booker and R. L. Klueh

ABSTRACT

Filler metal of AWS A5.14 Class ERNiCr-3 (67% Ni-20% Cr-3% Mn-2.5% Nb), often known as Inconel 82, is conventionally used for austenitic-to-ferritic dissimilar-metal transition weld joints. For example, this filler metal is proposed for use in the transition joints for the steam generator system of the Clinch River Breeder Reactor Plant. The potentially serious consequences of failures in transition joints make necessary a detailed understanding of their behavior. Such an understanding requires, among other things, a thorough knowledge of the mechanical properties of the materials involved. This report describes recent efforts to develop analytical descriptions of the creep and creep-rupture behavior of ERNiCr-3 weld metal. These results are compared with previous analyses of the behavior of 2 1/4 Cr-1 Mo steel and alloy 800H, the two base metals that would be joined by the ERNiCr-3 filler metal in one of the proposed CRBRP transition joints.

INTRODUCTION

Filler metal of AWS A5.14 Class ERNiCr-3 (67% Ni-20% Cr-3% Mn-2.5% Nb), often known as Inconel 82, is conventionally used for austenitic-to-ferritic dissimilar-metal transition weld joints. For example, this filler metal is proposed for use in the transition joints for the steam generator system of the Clinch River Breeder Reactor Plant (CRBRP). A cross section of the proposed joint is shown schematically in Fig. 1. The other weld filler metal shown is 16-8-2 (16% Cr-8% Ni-2% Mo-bal Fe) stainless steel. Alloy 800H is used as a spool piece to provide a gradual transition of thermal expansion coefficients across the weldment and thus lower projected thermal stresses.

---

*Work performed under DOE/RRT 189a 0H103, Piping and Fittings Development.

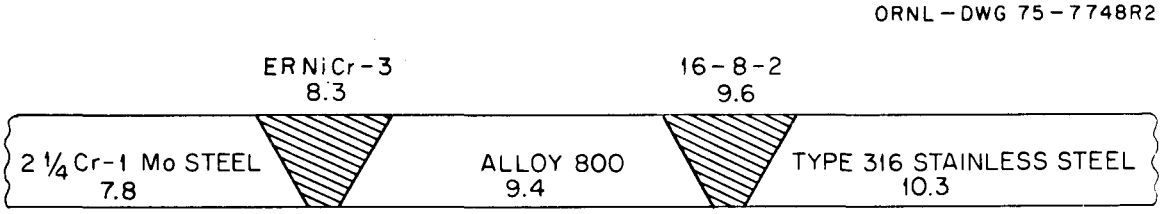

Fig. 1. Proposed CRBRP Transition Joint Configuration. Mean coefficients of expansion from room temperature to 538°C (1000°F) are noted below each material.

The potentially serious consequences of failures in transition joints demand a detailed understanding of their behavior. Such an understanding requires, among other things, a thorough knowledge of the mechanical properties of the materials involved. This report describes recent efforts to develop analytical descriptions of the creep and creep-rupture behavior of ERNiCr-3 weld metal. These results will be compared with previous analyses[1-4] of the behavior of 2 1/4 Cr-1 Mo steel and alloy 800H, the two base metals that would be joined by the ERNiCr-3 filler metal in one of the proposed CRBRP transition joints.

MATERIAL

The weld metal tested to obtain the data analyzed herein is fully characterized elsewhere.[5,6] Briefly, welds were made either between two 19-mm-thick plates of 2 1/4 Cr-1 Mo steel or between 13-mm-thick plates of 2 1/4 Cr-1 Mo steel and alloy 800H. The smaller welds were made with cold-wire filler metal and a 90°-included-angle V-groove geometry that required a root pass and seven fill passes. The larger welds were made with a 30°-included-angle V-groove joint geometry with a 32-mm root opening and a backing strip. Both hot- and cold-wire filler metal were used, the cold-wire requiring about 40 passes and the hot-wire 16 to 18. Table 1 shows the chemical compositions from a large and a small weld, along with AWS and ASTM specified limits for ERNiCr-3. As a result of base metal dilution, the small weld contained a higher iron concentration. No effect on creep properties was noted, however. All welds were radiographed, and no defects were detected. Creep-rupture test specimens

Table 1. Chemical Composition of ERNiCr-3 Filler Metal

Element	Chemical Composition, wt %		
	Small Weldment	Large Weldment	ASTM B304 AWS A5.14
Ni	Balance	Balance	67.0 min
Cu		0.3	0.5 max
Mn	2.7	2.0	2.5-3.5
Fe	10	2.8	3.0 max
Si		0.2	0.5 max
C	0.03	0.02	0.1 max
S			0.015 max
Ti	0.3	0.41	0.75 max
Nb	1.8	1.8	2.0-3.0
Cr	18.0	19.5	18-22

were longitudinal all-weld-metal buttonhead specimens with a 3.18-mm-diam (0.125-in.) by 28.6-mm-long (1.125-in.) gage section.

QUALITATIVE DESCRIPTION OF BEHAVIOR

Features of the creep behavior of ERNiCr-3 weld metal are described in detail elsewhere.[5,6] First, as can be seen in Figs. 2 and 3, the material behaves differently in the ranges 454 to 566°C (850–1050°F) and 621 to 732°C (1150–1350°F). As seen in the figures, logarithmic plots of stress against rupture life or minimum creep rate appeared quite different in these two regimes. The creep curves also appear different in the two temperature regions. At the low temperatures (Fig. 4), and especially at low stresses, the curves were characterized by a high initial creep rate followed by a rapid transient during which the creep rate decreased to a "steady state." Once the steady state was reached, it was maintained almost to failure. That is, these tests showed essentially no tertiary creep. At the highest stresses the transition from the primary to the secondary stage was not as abrupt.

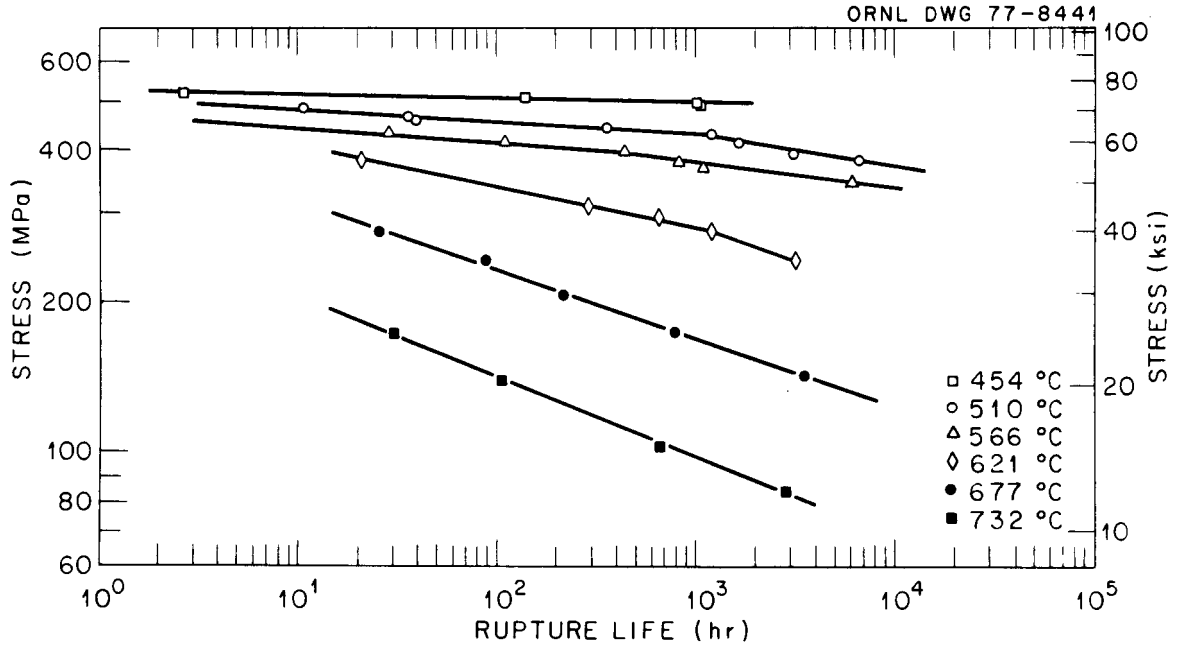

Fig. 2. Creep-Rupture Curves for ERNiCr-3 Weld Metal. Lines were visually fitted to the data.

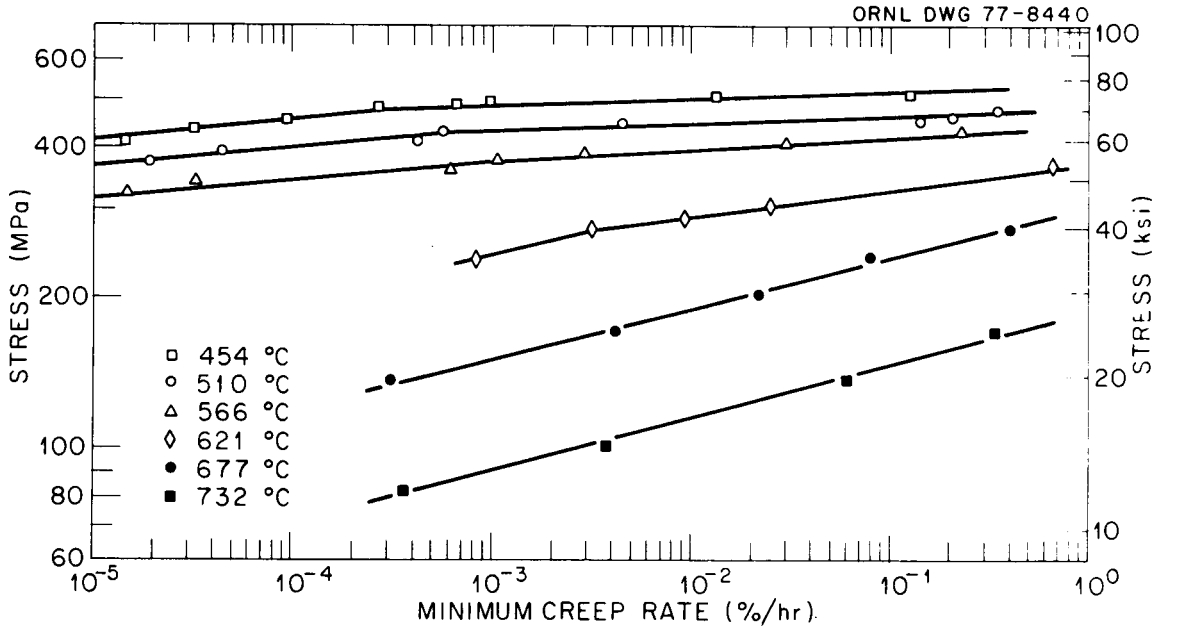

Fig. 3. Relationship Between Stress and Minimum Creep Rate for ERNiCr-3 Weld Metal. Lines were visually fitted to the data.

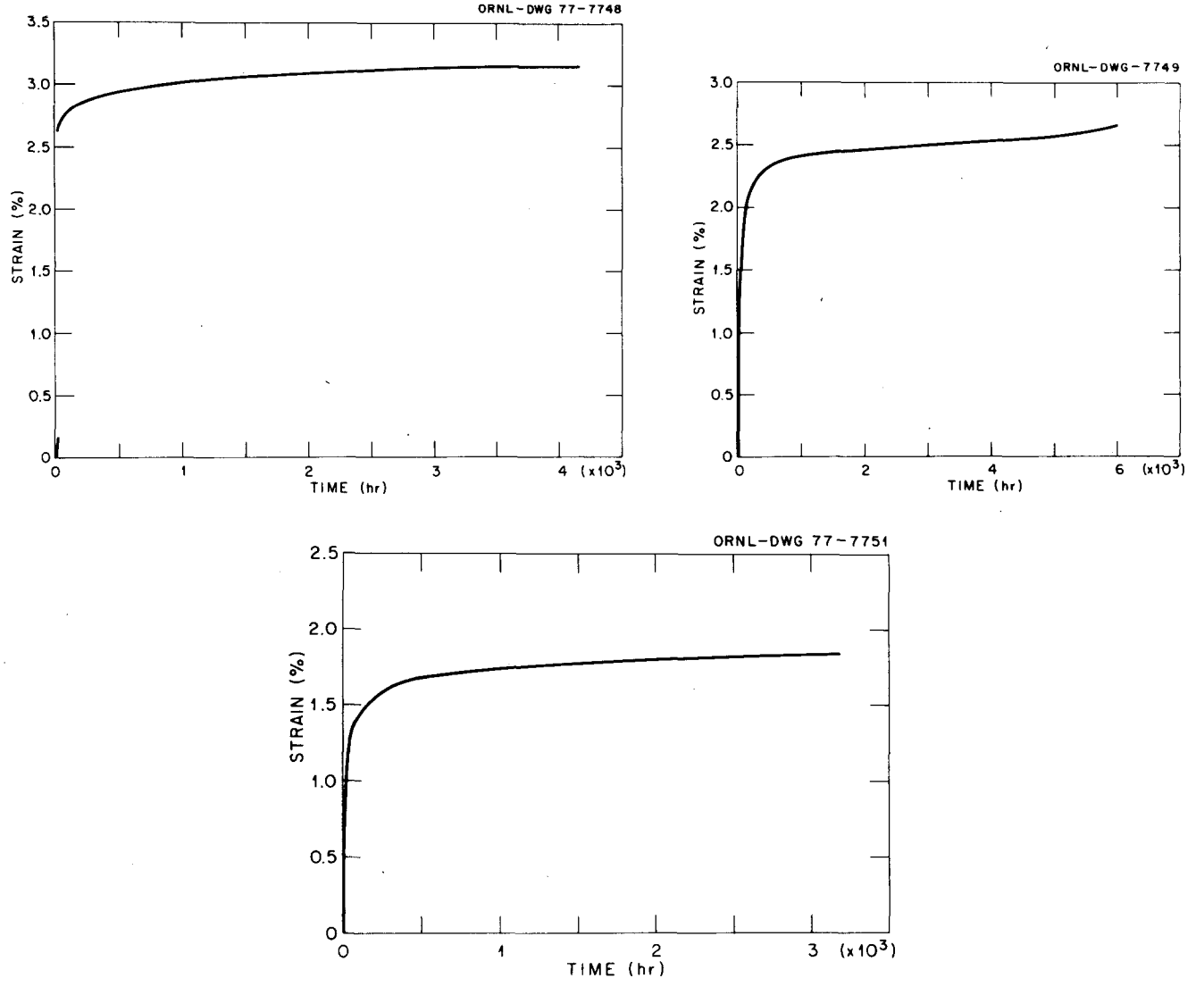

Fig. 4. Example of Creep-Curve Shape at (a) 454°C and 413 MPa, (b) 510°C and 327 MPa, and (c) 566°C and 327 MPa.

At the two highest temperatures (677 and 732°C), the creep curves were characterized by very little primary creep (Fig. 5). Rather quickly the test was in the steady state, which was not as long as it was at the lower temperatures. These curves had well-defined tertiary stages. Finally, the curve shapes at 621°C (Fig. 6) appeared to fall between those at the low temperatures and at 677 and 732°F.

In general, the total elongations and reductions of area were consistent at all temperatures.[5,6] Except at 454°C, both decreased with decreasing stress (increasing rupture life). At 454°C there was little change in ductility over the range of stresses tested. It is interesting to note that at the high temperatures the tests at 621°C had the least elongation.

Several specimens ruptured prematurely at 454, 510, and 566°C.[5,6] Also noted was another peculiarity at these temperatures that can be described as an "instantaneous elongation," a "strain burst," or a "spontaneous deformation." The phenomenon exhibited itself in the form of a jump in the creep curves, examples of which are shown in Figs. 7 through 9. These "strain bursts" appeared at different times in the creep process: shortly after loading during primary creep (Fig. 7) and during secondary creep (Fig. 8). Single (Fig. 8) and multiple (Fig. 9) bursts were observed; when the burst occurred early in the creep test (Fig. 7), it was difficult to determine whether it was single or multiple.

The phenomenon was quite general at 454 and 510°C, where essentially all tests displayed one or more strain bursts during the course of the test. Only a few tests displayed the phenomenon at 566°C, and no strain bursts were seen at 621, 677, and 732°C. Strain burst magnitudes ranged from strains of about 0.1% up to greater than 6%. When the strain burst occurred during the steady-state stage, the creep rate after the burst was usually little different from before (Fig. 9).

There is no direct evidence to link the strain burst phenomenon with the observations of premature failure. The fact that both phenomena occurred only in the low-temperature tests could signify a relationship, as if a premature failure occurred during a strain burst of magnitude greater than the ductility of the alloy. However, such a relationship cannot be verified from the current data.

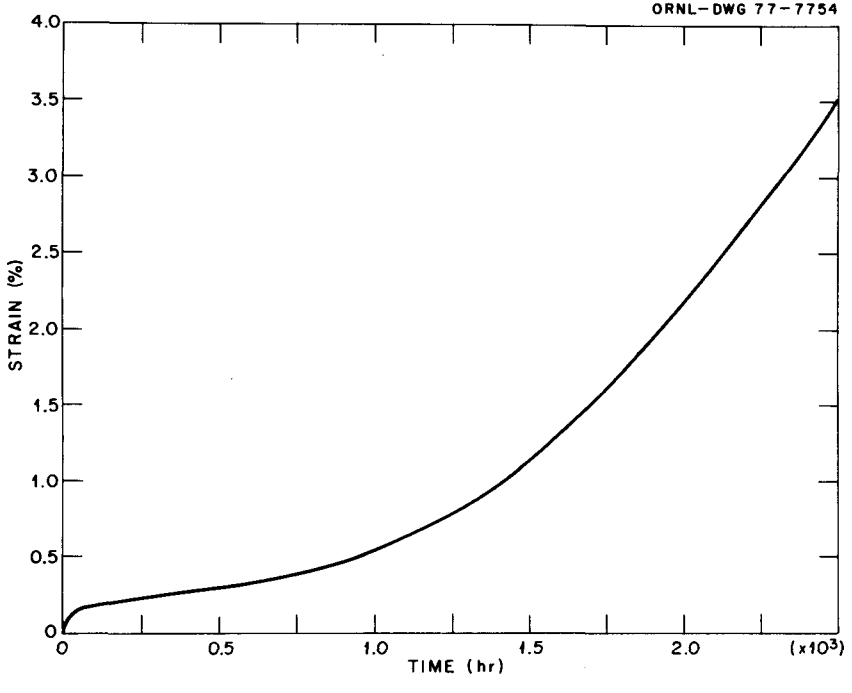

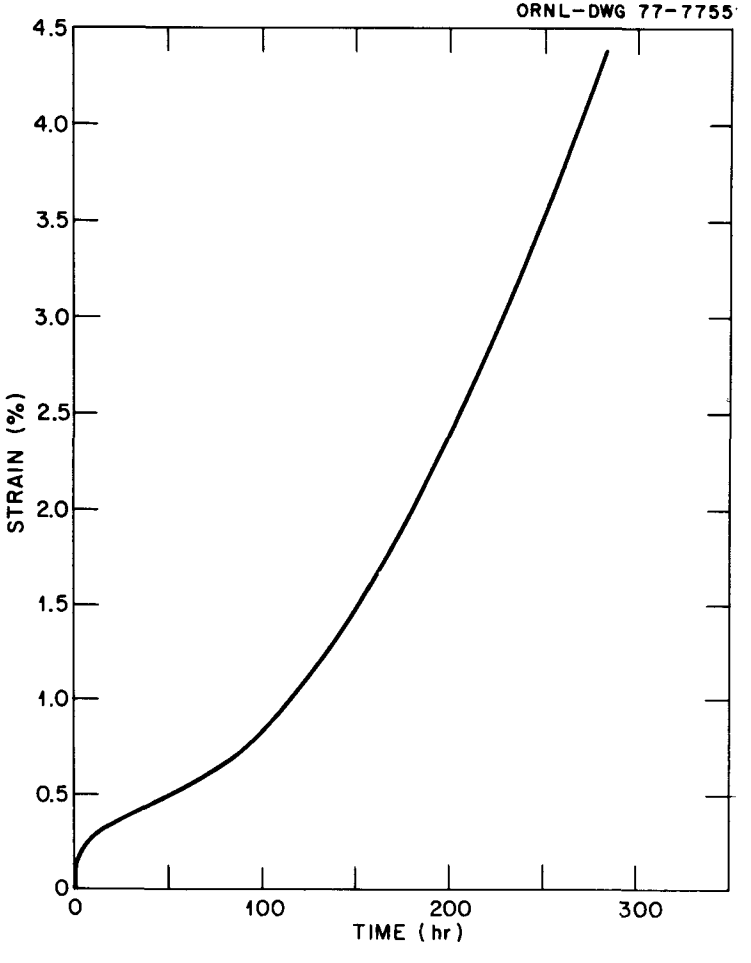

Fig. 5. Example of Creep-Curve Shape at (a) 677°C and 138 MPa and (b) 732°C and 103 MPa.

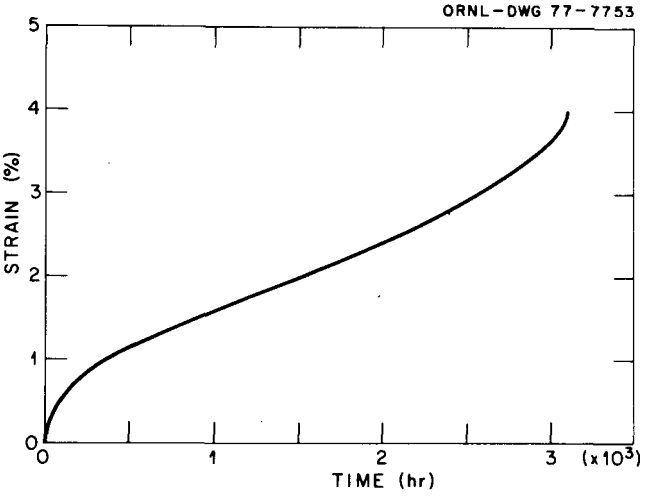

Fig. 6. Example of Creep Curve Shape at 621°C and 241 MPa.

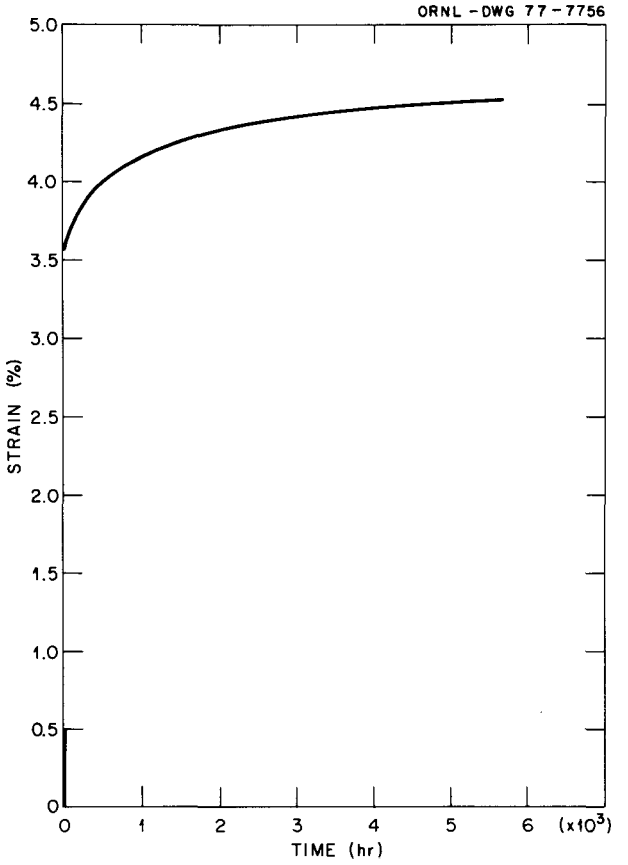

Fig. 7. Example of "Instantaneous Elongation" or a "Strain Burst" during Primary Creep in ERNiCR-3 Weld Metal Tested at 454°C and 434 MPa.

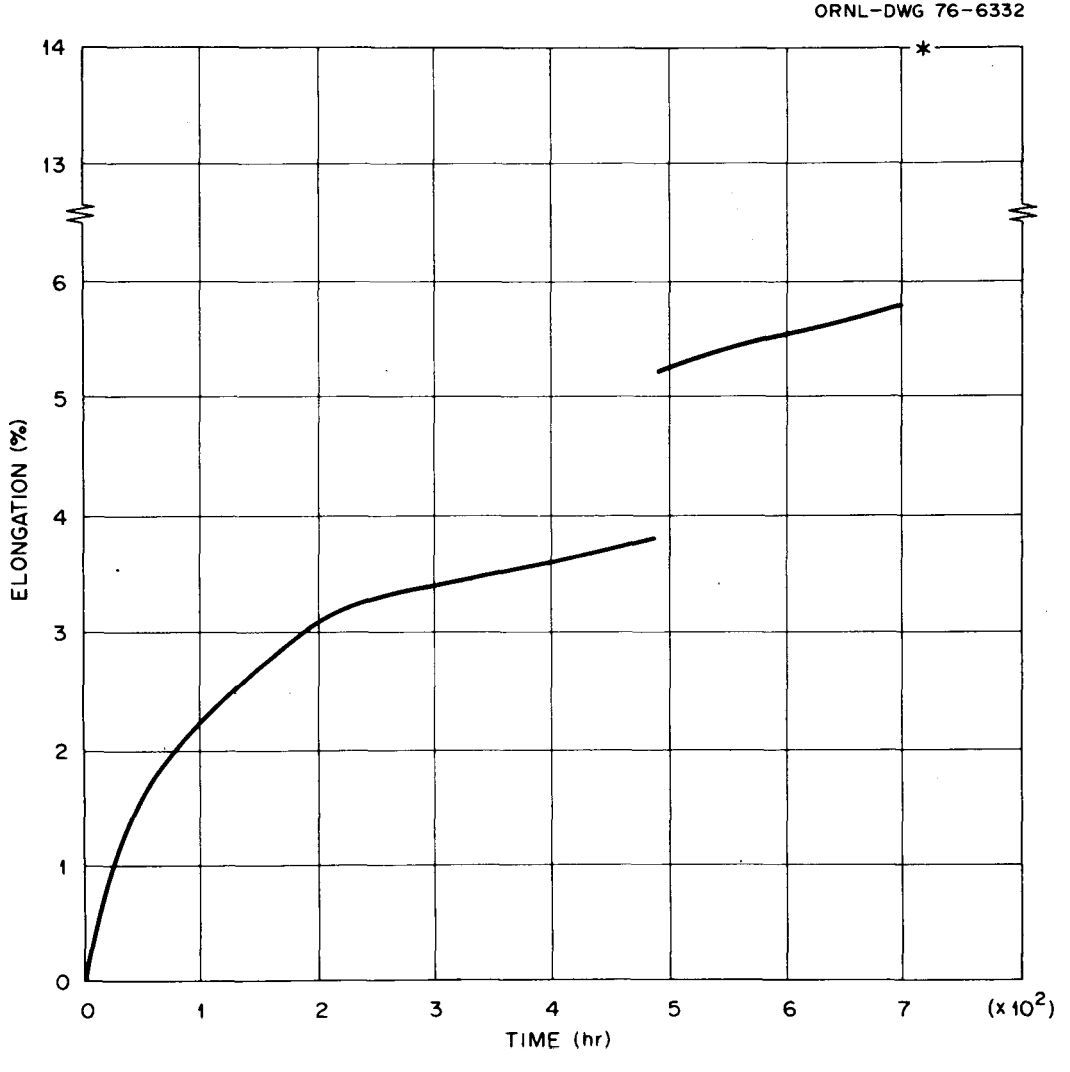

Fig. 8. Example of a "Strain Burst" During Secondary Creep Stage of ERNiCr-3 Weld Metal Tested at 454°C and 496 MPa.

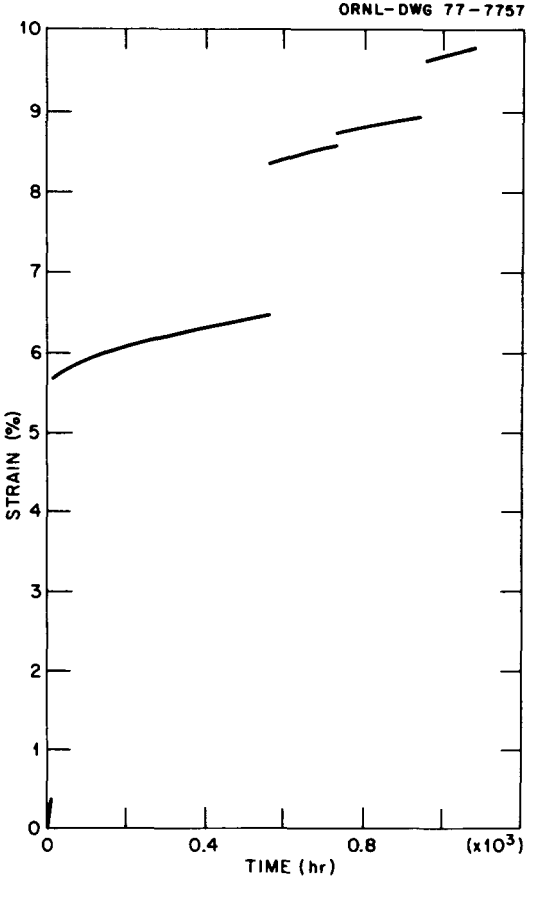

Fig. 9. Example of Multiple "Strain Bursts" in ERNiCr-3 Weld Metal Tested at 454°C and 489 MPa.

The occurrence or magnitude of strain bursts could not be predicted analytically from available data. All analyses described in this report were performed on creep curves from which the strain bursts had been graphically removed by simple vertical shifts of the curve segments to obtain continuous curves.

ANALYTICAL RESULTS

Analysis of the available data consisted of two parts: description of trends in the data themselves and extrapolation of results to longer times and lower stresses more relevant to design applications. As will become evident, these two aspects can present totally different problems for this material, so each will be discussed separately.

Description of Data Trends

For reasons noted above, the available data were analyzed in two separate sets — low-temperature data (454-566°C) and high-temperature data (621-732°C). The data used are tabulated in the Appendix. Data from hot- and cold-wire welds were analyzed as functions of stress, σ (MPa), and temperature, T (K) by use of a generalized regression approach.[7] Figures 10 through 13 compare the results of these analyses with experimental data. The data were described by

Low Temperature:

$$\log \dot{e}_m = 232.79 - 265660/T - 76.95 \log \sigma + \frac{91102}{T} \log \sigma \ , \qquad (1)$$

$$\log t_r = -120.56 + 142580/T + 39.91 \log \sigma - \frac{48753}{T} \log \sigma \ ; \qquad (2)$$

High Temperature:

$$\log \dot{e}_m = 55.44 - 76585/T - 10.12 \log \sigma + \frac{19320}{T} \log \sigma \ , \qquad (3)$$

$$\log t_r = -53.69 + 68758/T + 13.33 \log \sigma - \frac{19390}{T} \log \sigma \ . \qquad (4)$$

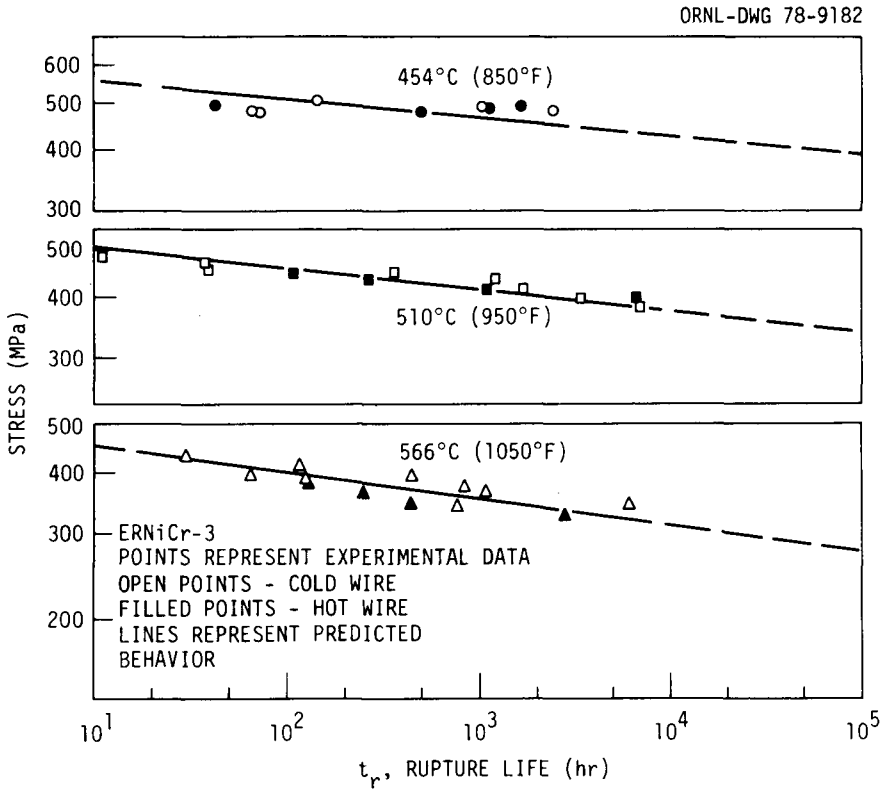

Fig. 10. Comparison of Predicted and Experimental Stress-Rupture Behavior of ERNiCr-3 Weld Metal at 454°C, 510°C, and 566°C.

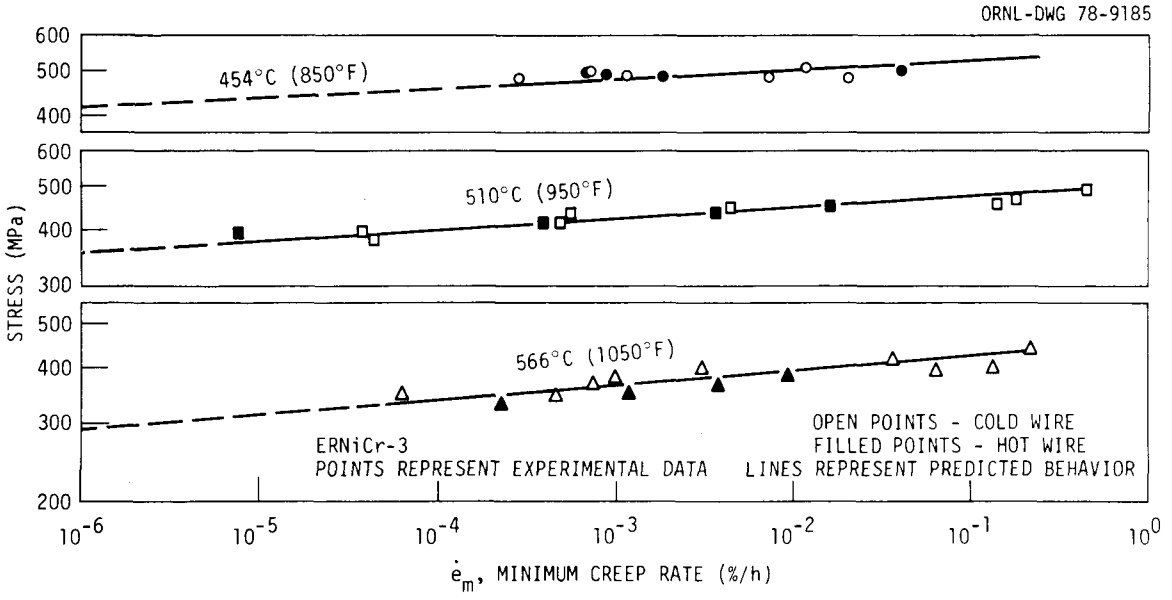

Fig. 11. Comparison of Predicted and Experimental Minimum Creep Rates of ERNiCr-3 Weld Metal at 454°C, 510°C, and 566°C.

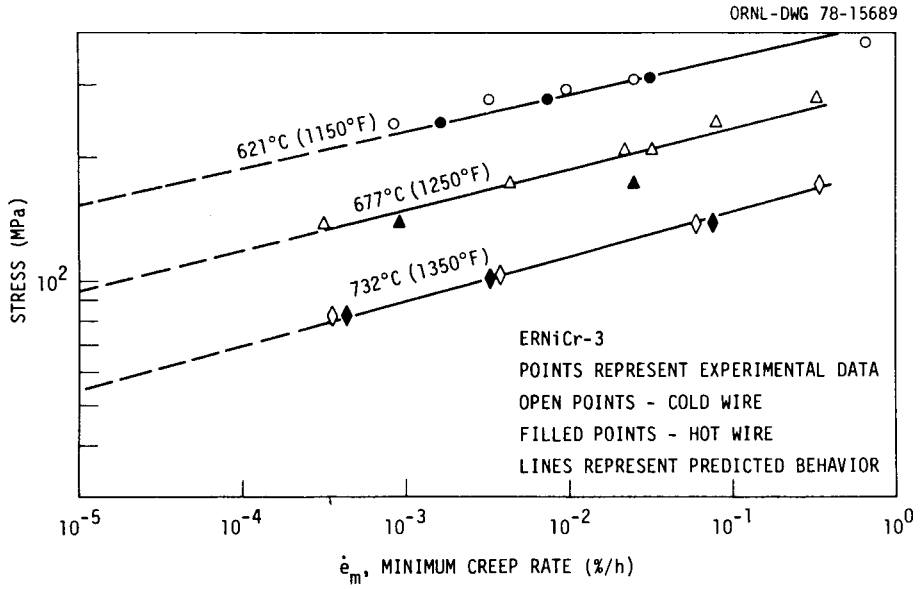

Fig. 12. Comparison of Predicted and Experimental Stress-Rupture Behavior of ERNiCr-3 Weld Metal from 621 to 732°C.

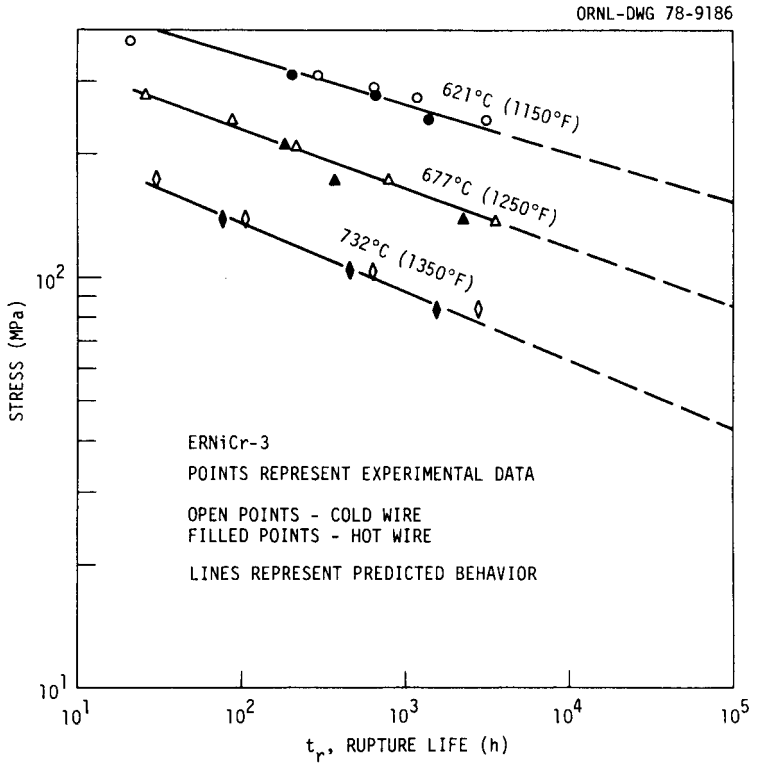

Fig. 13. Comparison of Predicted and Experimental Minimum Creep Rates of ERNiCr-3 Weld Metal from 621 to 732°C.

Table 2 summarizes the fits of these equations to the data. Note that all four equations are of the same form, predicted log σ-log t_r (or log $\dot{e}_m$) isotherms being linear, with slopes varying linearly with $1/T$.

Table 2. Summary of Fits to Data for Minimum Creep Rate ($\dot{e}_m$) and Rupture Life (t_r)

Equation	Dependent Variable	Temperature Range (°C)	Number of Data	R^2 (%)[a]	SEE[b]
(1)	log $\dot{e}_m$	454-566	34	73.4	0.65
(2)	log t_r	454-566	34	62.6	0.47
(3)	log $\dot{e}_m$	621-732	23	94.1	0.26
(4)	log t_r	621-732	23	94.9	0.16

[a]Coefficient of Determination. The value of R^2 (%) gives the percentage of variation in the data described by a given model.

[b]Standard error of estimate in terms of the dependent variable.

Next we examined trends in data for the time and creep strain to the onset of tertiary creep, using methods developed previously[8-12] for several other materials. As shown in Fig. 14, two definitions of the onset of tertiary creep were used. The time t_{ss} and strain e_{ss} correspond to values obtained with a 0.2% offset from the linear secondary creep portion of the creep curve. The time t_2 and strain e_2 correspond to values visually obtained at the first deviation from linear secondary creep.

In the temperature range from 454 to 566°C, there was essentially no tertiary creep portion, with rupture occurring very quickly after deviation from linear creep. In this regime t_2 and t_{ss} are essentially equal, and either can be described by

$$t_{ss} = t_2 = 0.98 t_r \ , \tag{5}$$

as shown in Fig. 15.

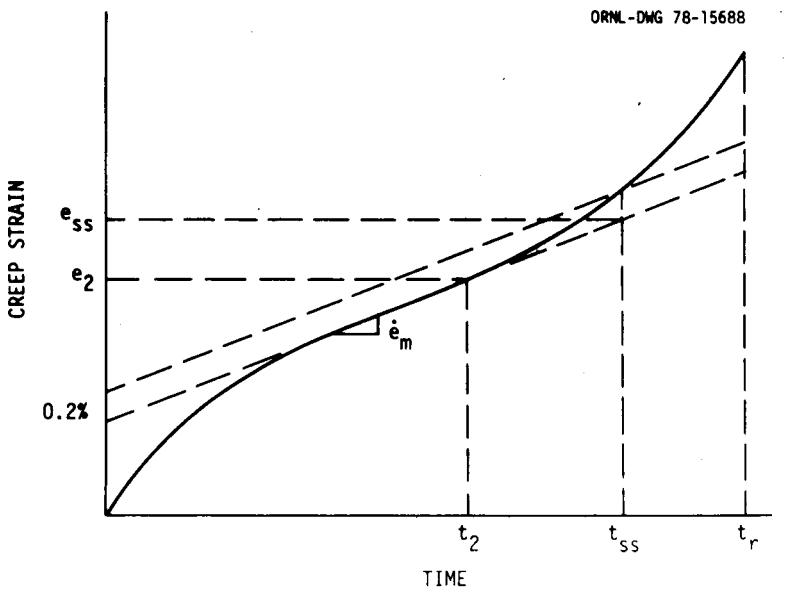

Fig. 14. Schematic Definition of the Onset of Tertiary Creep.

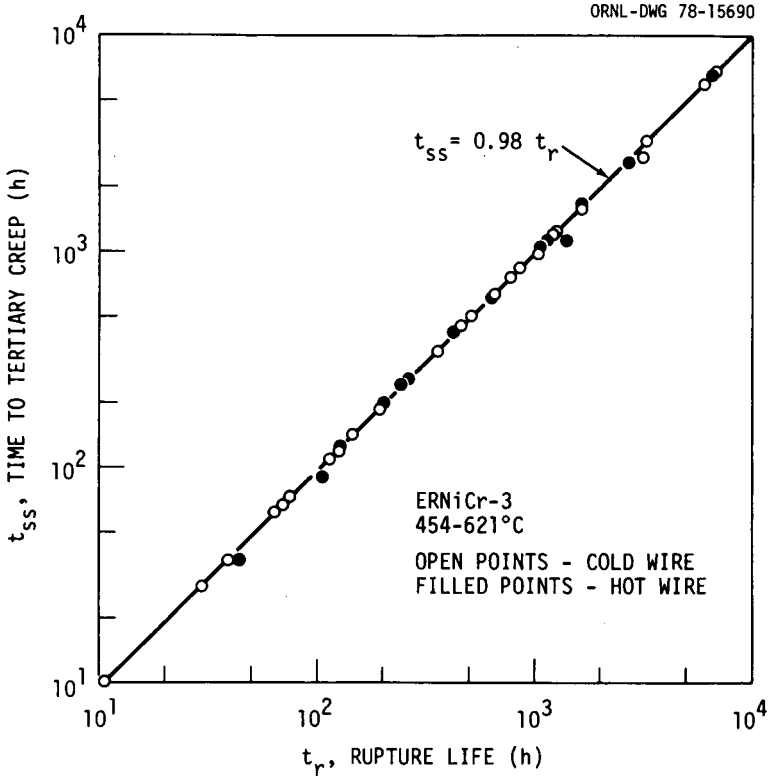

Fig. 15. Relationship Between Rupture Life and Time to Tertiary Creep (0.2% Offset) from 454 to 621°C.

Data for t_{ss} in the range 677-732°C showed curvature when plotted log-log against t_r (Fig. 16). This phenomenon can be attributed to the shapes of the creep curves in this range. As times become longer the creep strain to tertiary creep becomes smaller, and the constant 0.2% offset becomes relatively larger. As a result t_{ss} becomes a larger and larger fraction of t_r. When viewed in terms of t_2, these plots are again essentially linear, with the behavior being described by

$$t_2 = 0.035 t_r^{1.20} , \tag{6}$$

as shown in Fig. 17. This equation will eventually yield $t_2 > t_r$ at very long times. For the longest term available data $t_2 \approx 0.2 t_r$. Thus

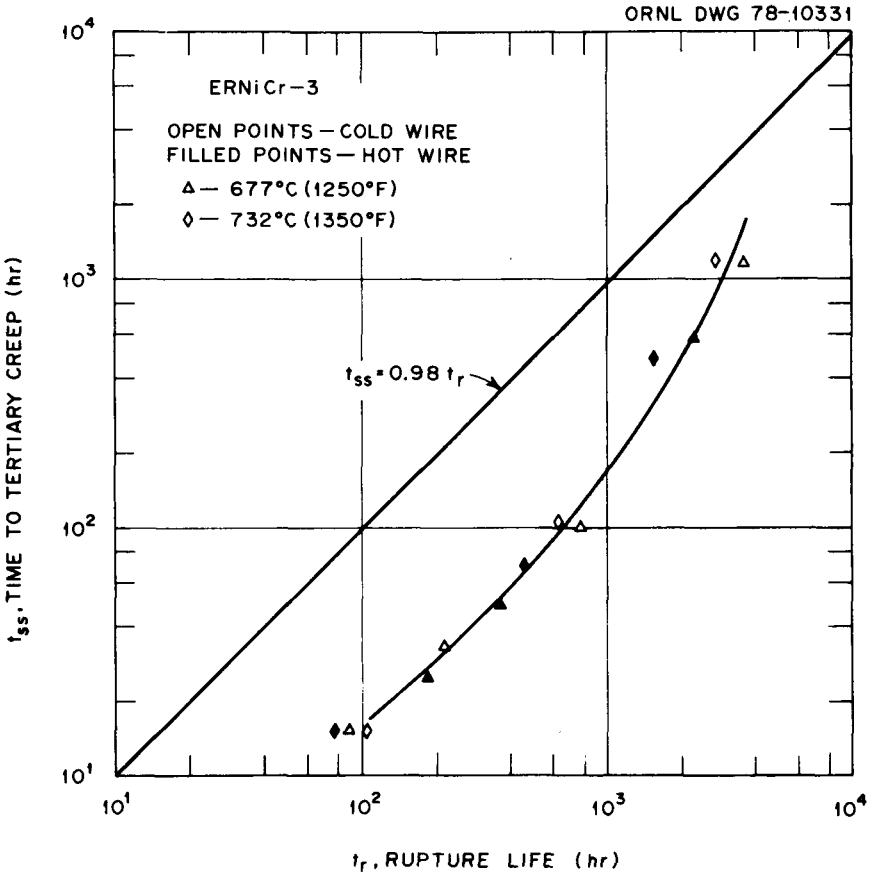

Fig. 16. Relationship Between Rupture Life and Time to Tertiary Creep (0.2% Offset) at 677 and 732°C.

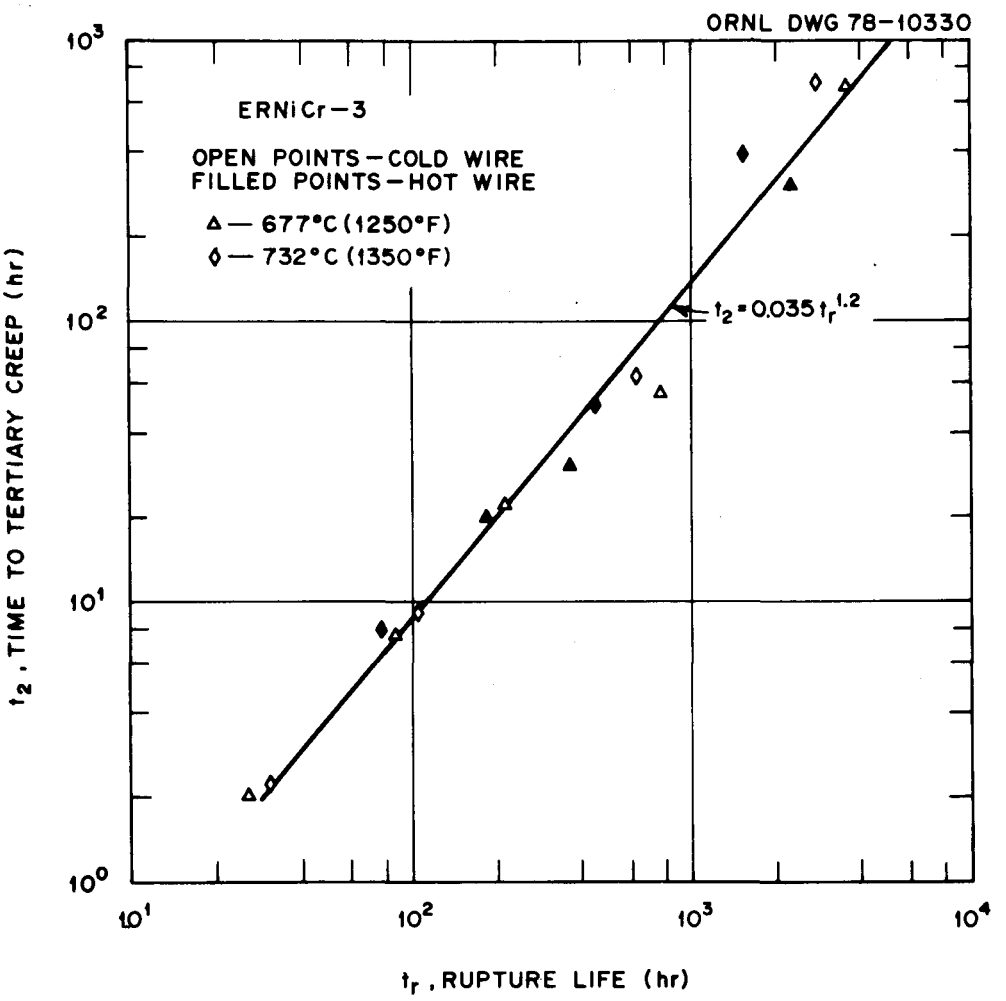

Fig. 17. Relationship Between Rupture Life and Time to Tertiary Creep at 677 and 732°C.

we (arbitrarily) recommend predicting t_2 by Eq. (6) or by $t_2 = 0.6t_r$, whichever is smaller, since $0.6t_r$ falls midway between $0.2t_r$ and t_r, the range in which t_2 must lie. At 621°C t_2 was given approximately by $0.85t_r$.

Data for the strain to tertiary creep were analyzed on the basis of the concept of average creep rates to tertiary creep, $\dot{e}_{ss} = e_{ss}/t_{ss}$ and $\dot{e}_2 = e_2/t_2$. In the range 454 to 566°C these average creep rates were described by the relationship

$$\dot{e}_2 = \dot{e}_{ss} = 0.84\dot{e}_m^{0.75} , \qquad (7)$$

while data in the range 621 to 732°C yielded the relationship

$$\dot{e}_2 = 1.5\dot{e}_m \ . \tag{8}$$

Figures 18 and 19 illustrate these trends. The strains e_{ss} and e_2 can then be calculated from $e_{ss} = \dot{e}_{ss} t_{ss}$ and $e_2 = \dot{e}_2 t_2$, yielding

$$e_{ss} = e_2 = 0.823 t_r \dot{e}_m^{0.75} \ (454\text{-}566°C) \ , \tag{9}$$

$$e_{ss} = e_2 = 1.28\dot{e}_m t_r \ (621°C) \ , \tag{10}$$

$$e_2 = 0.9\dot{e}_m t_r \text{ or } e_2 = 0.052\dot{e}_m t_r^{1.2} \ (677\text{-}732°C) \tag{11}$$

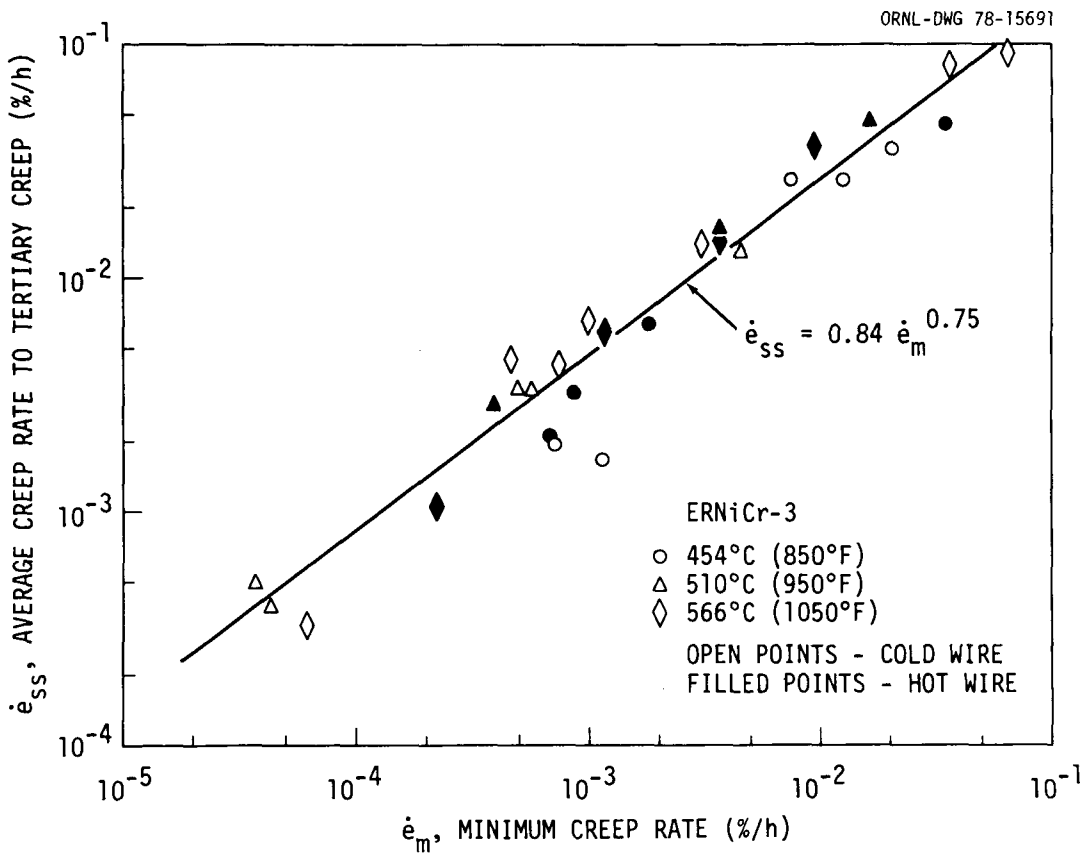

Fig. 18. Relationship Between Average Creep Rate to Tertiary Creep and Minimum Creep Rate for ERNiCr-3 Weld Metal from 454 to 566°C.

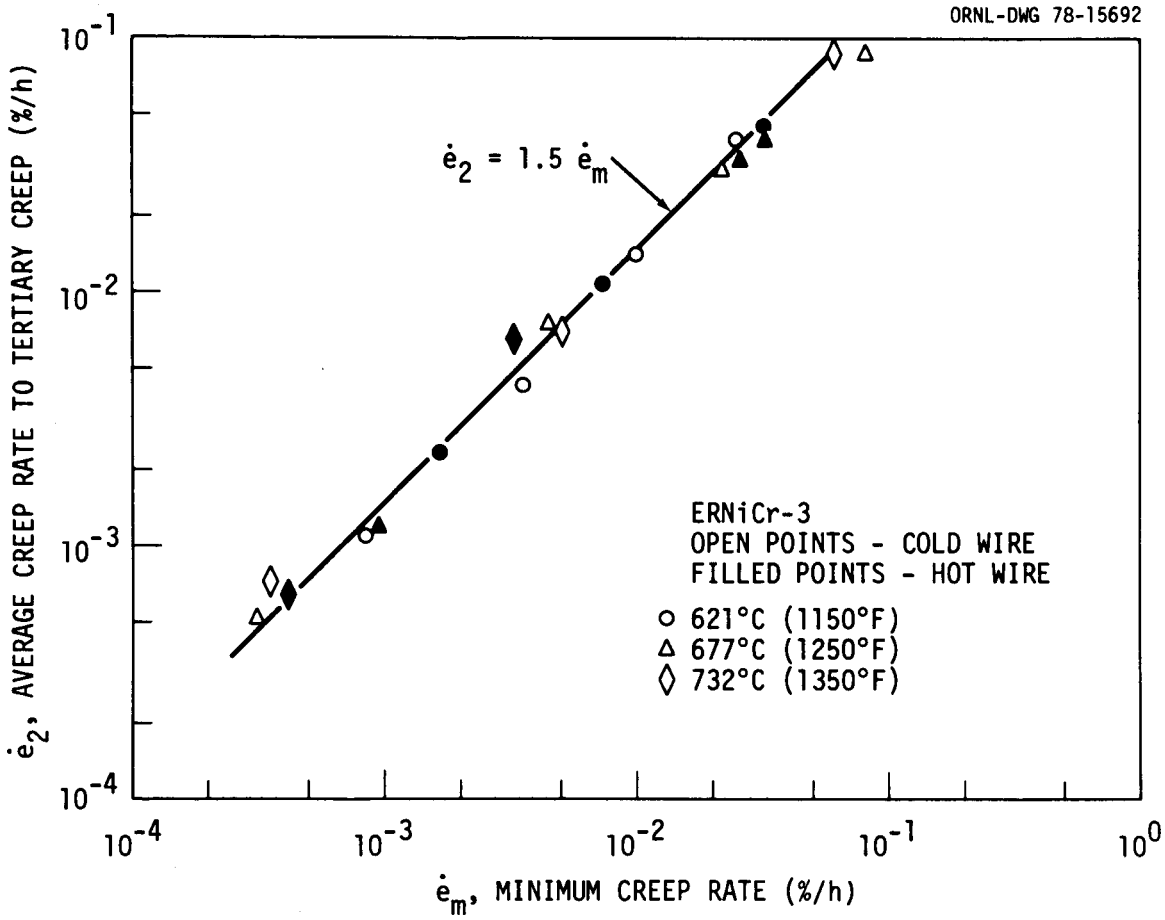

Fig. 19. Relationship Between Average Creep Rate to Tertiary Creep and Minimum Creep Rate for ERNiCr-3 Weld Metal from 621 to 732°C.

Figure 20 compares these predictions with available data, with $\dot{e}_m$ and t_r being predicted from Eqs. (1 through 4). Note that the data at 621°C show behavior intermediate between the low-temperature and high-temperature behavior. The predictions appear consistent with the trends in the data, although e_{ss} at 454°C is generally overestimated slightly, and e_2 at 732°C is generally underestimated slightly.

The final analysis required is the determination of the relationship between creep strain and time as a function of stress and temperature. A convenient means for viewing trends in creep curve shape involves the use of "normalized creep curves."[13] Creep curves are normally plotted in terms of creep strain, e, as a function of time, t. Tests at different stresses and temperatures can yield strains and times of widely varying

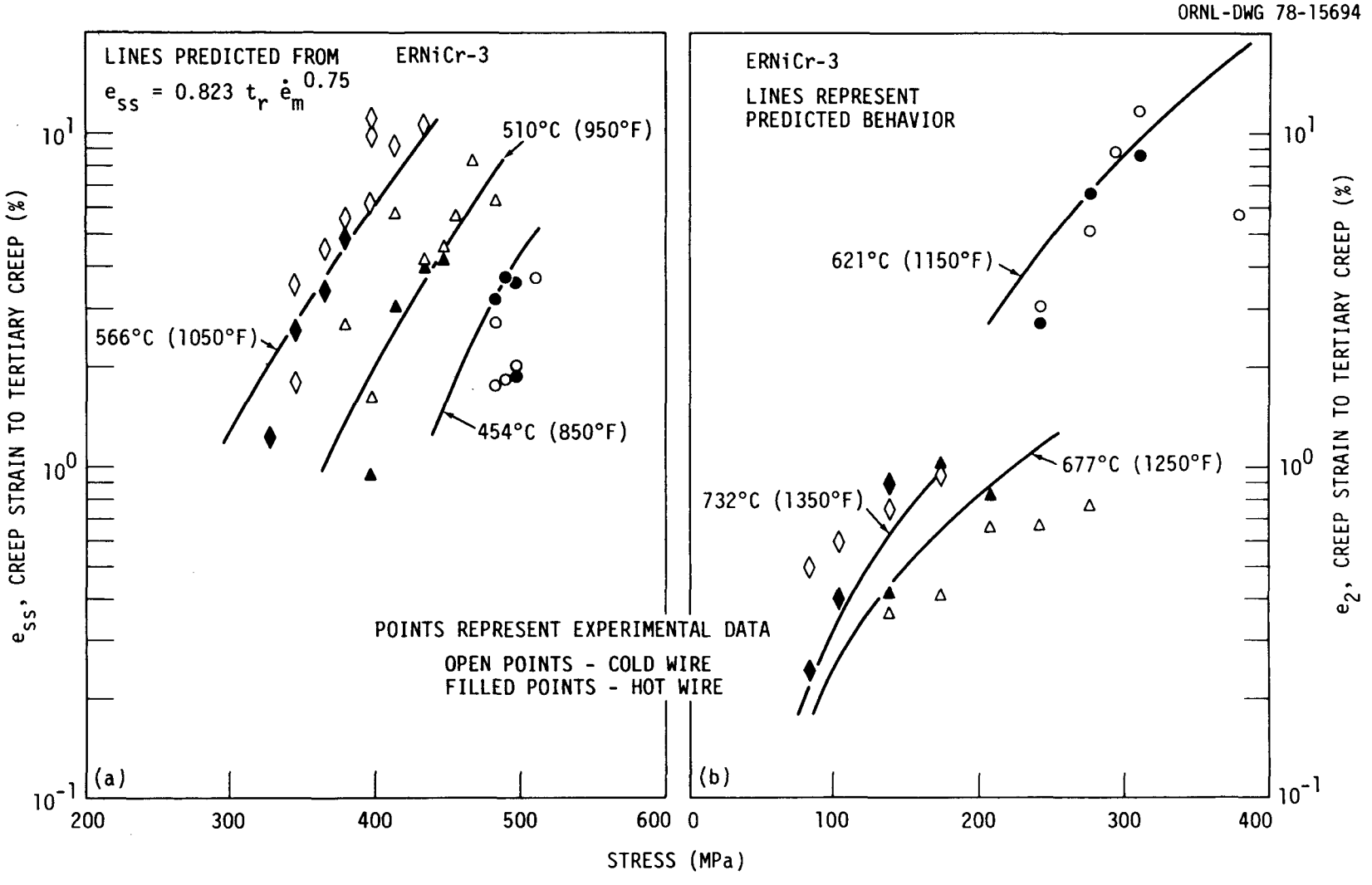

Fig. 20. Comparison of Predicted and Experimental Values for the Strain to the Onset of Tertiary Creep (a) from 454 to 566°C and (b) from 621 to 732°C.

magnitudes and thus are difficult to compare directly. One solution to this problem is to normalize all strains and times to a common scale.

The current data were examined by plotting normalized creep strain, e' (e/e_{ss} or e/e_2), versus normalized time, t' (t/t_{ss} or t/t_2). Thus, all curves fall on a single scale for t from 0 to the onset of tertiary creep with both values on axes ranging from 0 to 1.

The strain-time behavior was analyzed within the framework of the rational polynomial creep equation,[14] which has recently been used for a number of materials.[1-4,11,12] The equation is

$$e = \frac{Cpt}{1 + pt} + \dot{e}_m t \ , \tag{12}$$

where

e = creep strain,

t = time,

$\dot{e}_m$ = minimum creep rate, and

C = the limiting value of the transient primary creep strain.

The parameter p is related to the sharpness of the curvature of the primary creep region.

The properties of the rational polynomial creep equation given in Eq. (12) are reviewed in detail elsewhere[14] but will be briefly described here for completeness. Differentiating Eq. (12) one finds the creep rate, $\dot{e}_c$, is

$$\dot{e}_c = \frac{Cp}{(1 + pt)^2} + \dot{e}_m \ , \tag{13}$$

while the initial creep rate is given by

$$\dot{e}_0 = Cp + \dot{e}_m \ . \tag{14}$$

The parameter p is related to the rate of approach of the creep rate from $\dot{e}_0$ to $\dot{e}_m$. Figure 21 summarizes the properties of the rational polynomial equation.

Equation (12) can be rewritten in terms of the normalized creep coordinates as

$$e' = \frac{C'p't'}{1 + p't'} + \dot{e}'_m t' \ , \tag{15}$$

where

$$\dot{e}'_m = \dot{e}_m/\dot{e}_3 \ (\dot{e}_3 = \dot{e}_{ss} \text{ or } \dot{e}_3) \ , \tag{16}$$

$$C' = C/e_3 \ (e_3 = e_{ss} \text{ or } e_2) \ , \tag{17}$$

and

$$p' = pt_3 \ (t_3 = t_{ss} \text{ or } t_2) \ . \tag{18}$$

ORNL-DWG 76-3985R

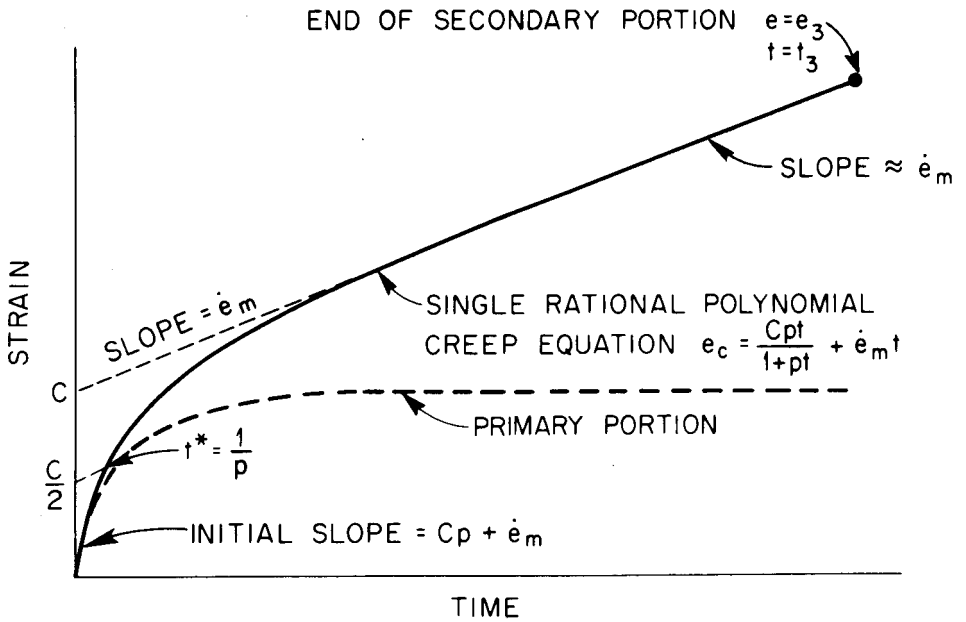

Fig. 21. Schematic Illustration of the Properties of the Rational Polynomial Creep Equation.

Note also that since $e' = 1$ at $t' = 1$,

$$C' = \frac{1 + p'}{p'} (1 - \dot{e}_m') \ , \tag{19}$$

reducing the number of independent equation parameters to two.

Equations (1) and (3) yield predictions for $\dot{e}_m$ that with Eq. (19) yield predictions for C, assuming p is known. As shown in Figs. 22 and 23, p can be related to the time to tertiary creep by

$$p = 6.5 t_{ss}^{-0.69} \ (454\text{-}566°C) \ , \tag{20}$$

and

$$p = 26/t_2 \ (621\text{-}732°C) \ . \tag{21}$$

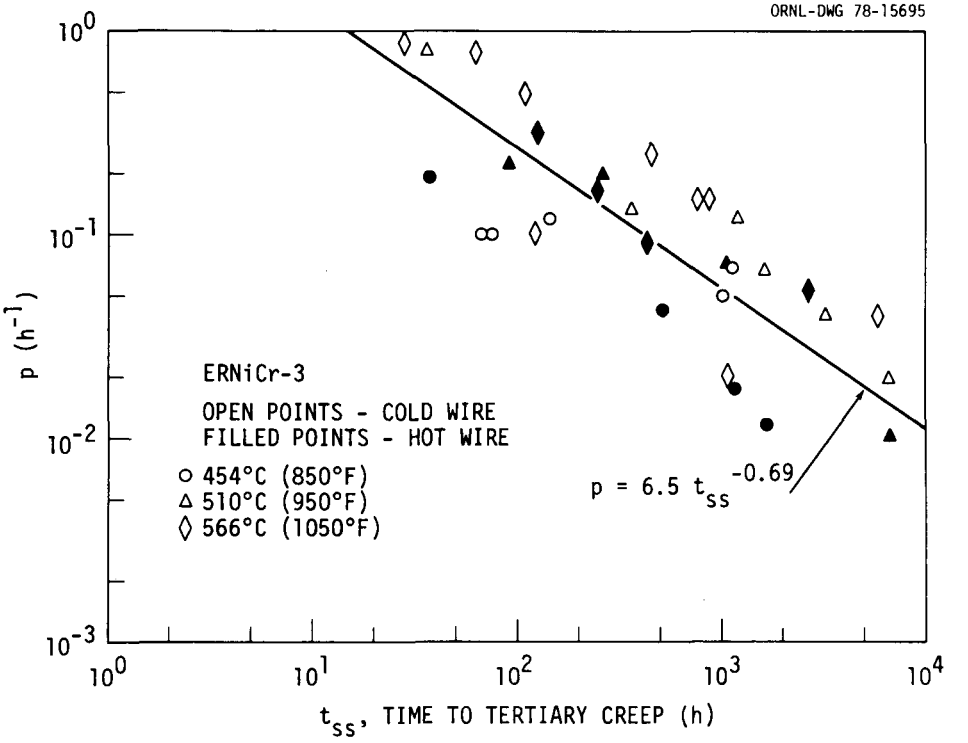

Fig. 22. Relationship Between Creep Parameter p and Time to the Onset of Tertiary Creep From 454 to 566°C.

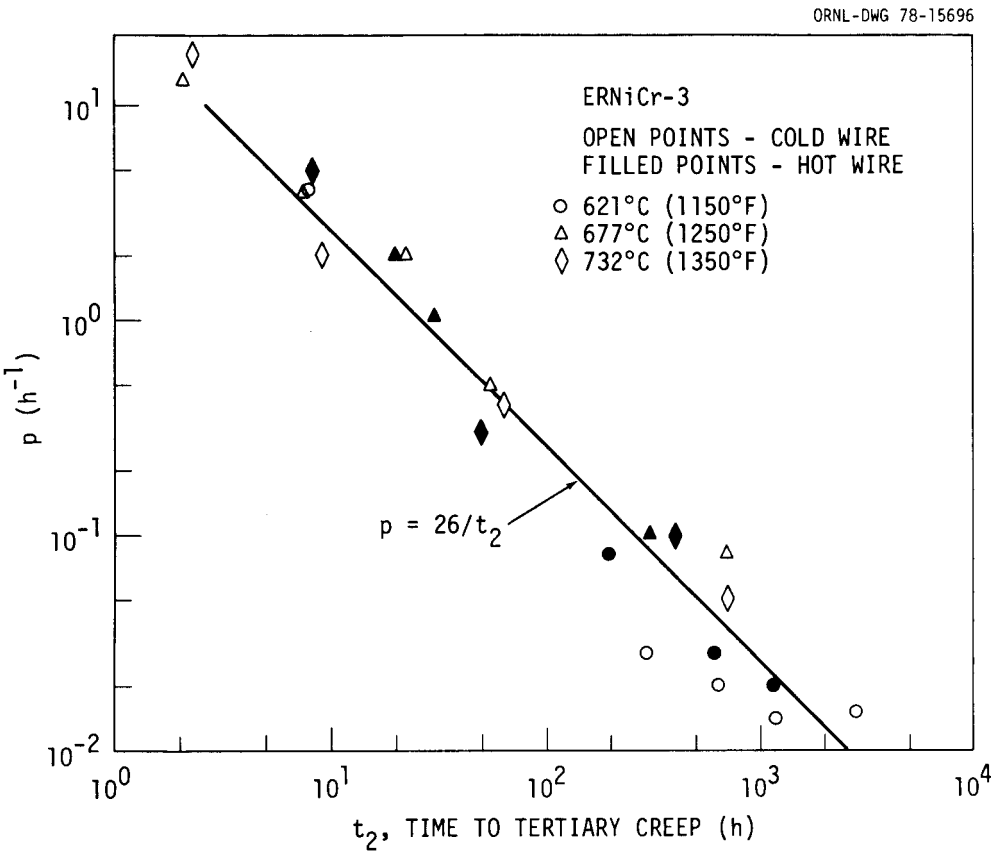

Fig. 23. Relationship Between Creep Parameter p and Time to the Onset of Tertiary Creep From 621 to 732°C.

Thus, the net effect of Eqs. (1 through 21) is to yield a comprehensive prediction of creep strain-time behavior up to the onset of tertiary creep, based on predictions for rupture life and minimum creep rate as functions of stress and temperature. Figures 24 through 29 compare predicted behavior with experimental creep curves. Shown are average, "upper limit," and "lower limit" predictions. Average predictions are based on $\dot{e}_m$ and t_r values calculated directly from Eqs. (1 through 4). Lower limit predictions are based on log t_r + 3SEE and log $\dot{e}_m$ - 3SEE (see Table 2) from Eqs. (1 through 4), while upper limit predictions are based on log t_r - 3SEE and log $\dot{e}_m$ + 3SEE from Eqs. (1 through 4). Figures 30 through 35 compare the predictions with the data in terms of normalized creep strain and time. Considering the uncertainties and scatter in the data themselves, the agreement between experimental and

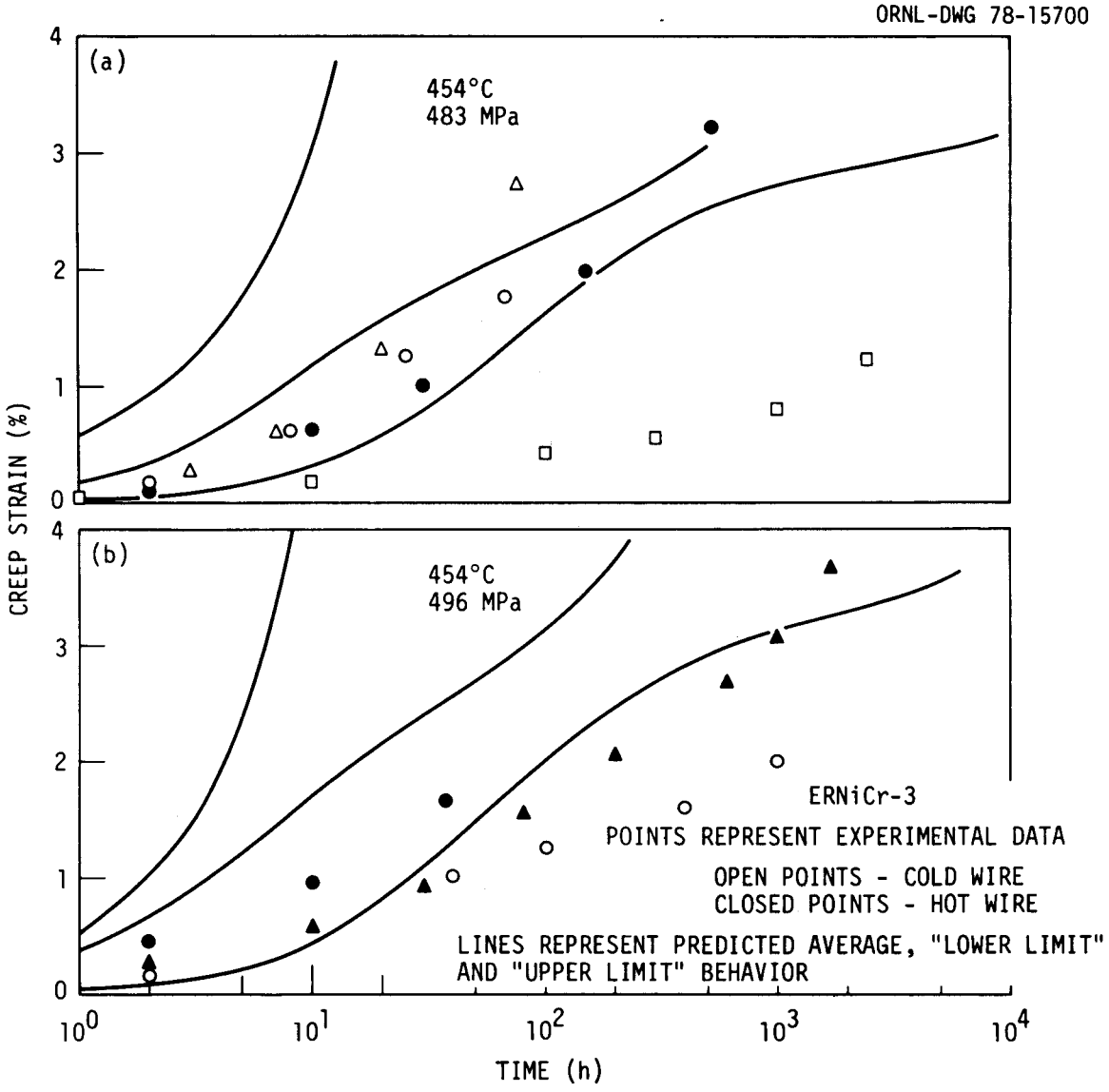

Fig. 24. Comparison of Predicted and Experimental Creep Behavior at 454°C.

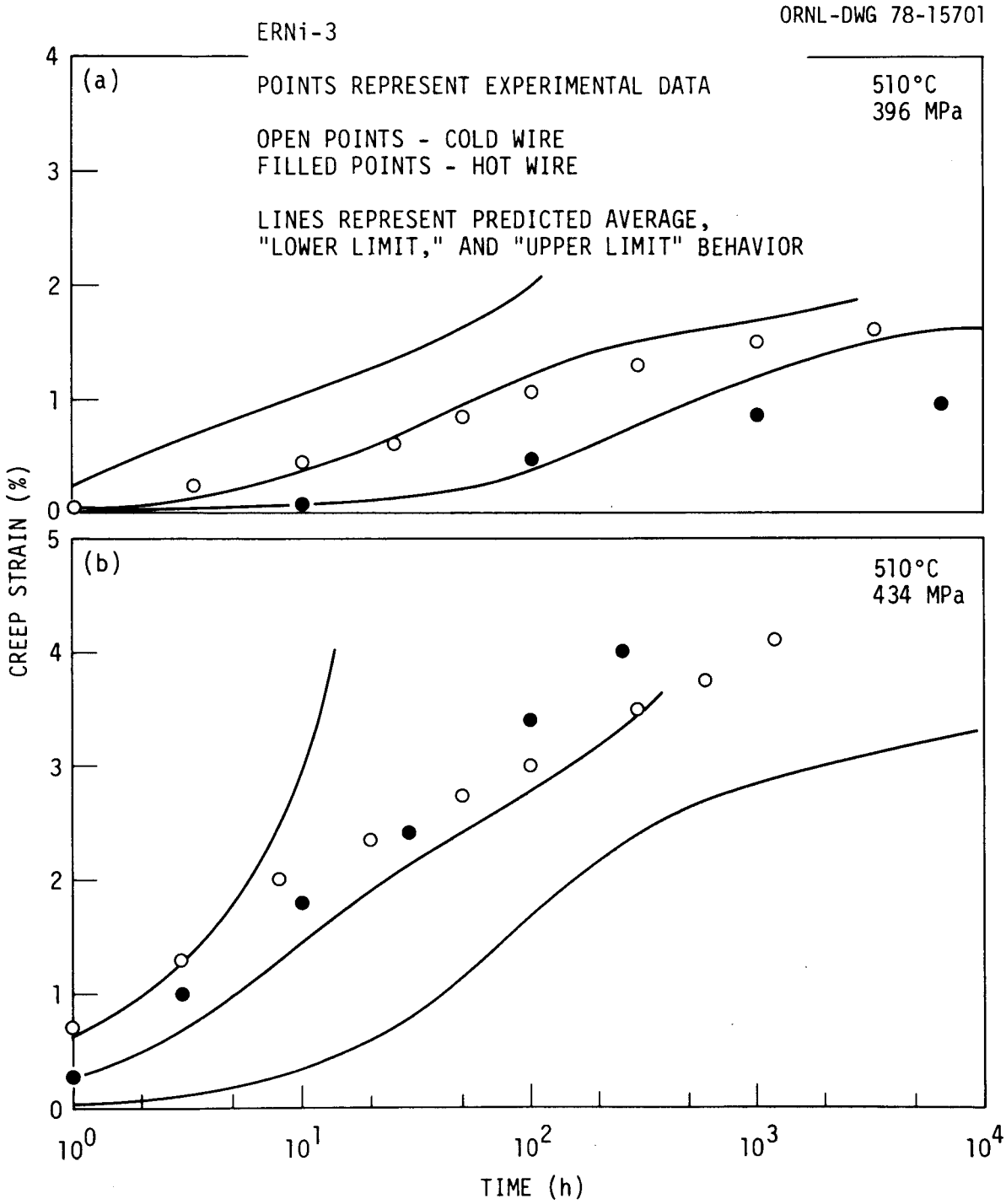

Fig. 25. Comparison of Predicted and Experimental Creep Behavior at 510°C.

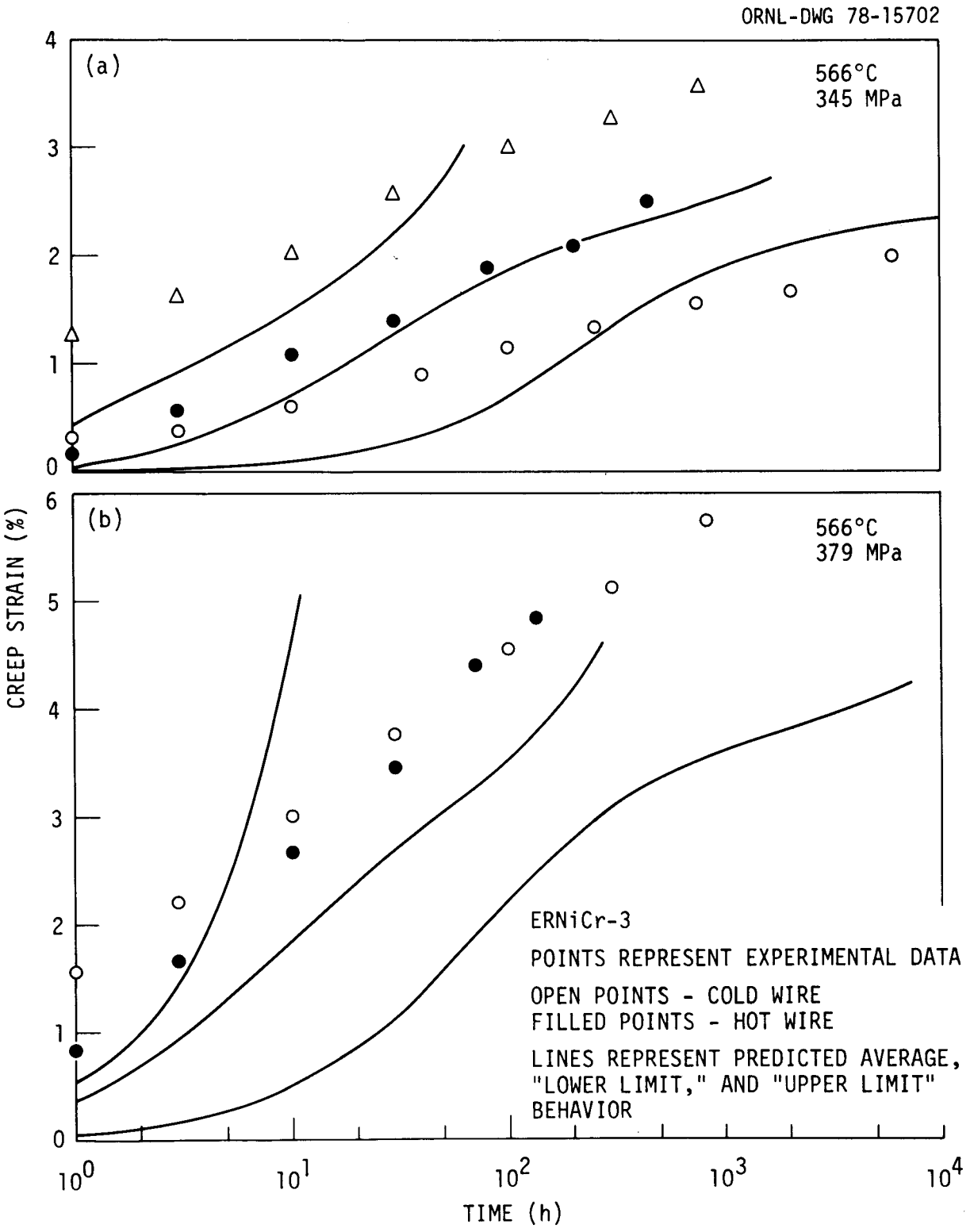

Fig. 26. Comparison of Predicted and Experimental Creep Behavior at 566°C.

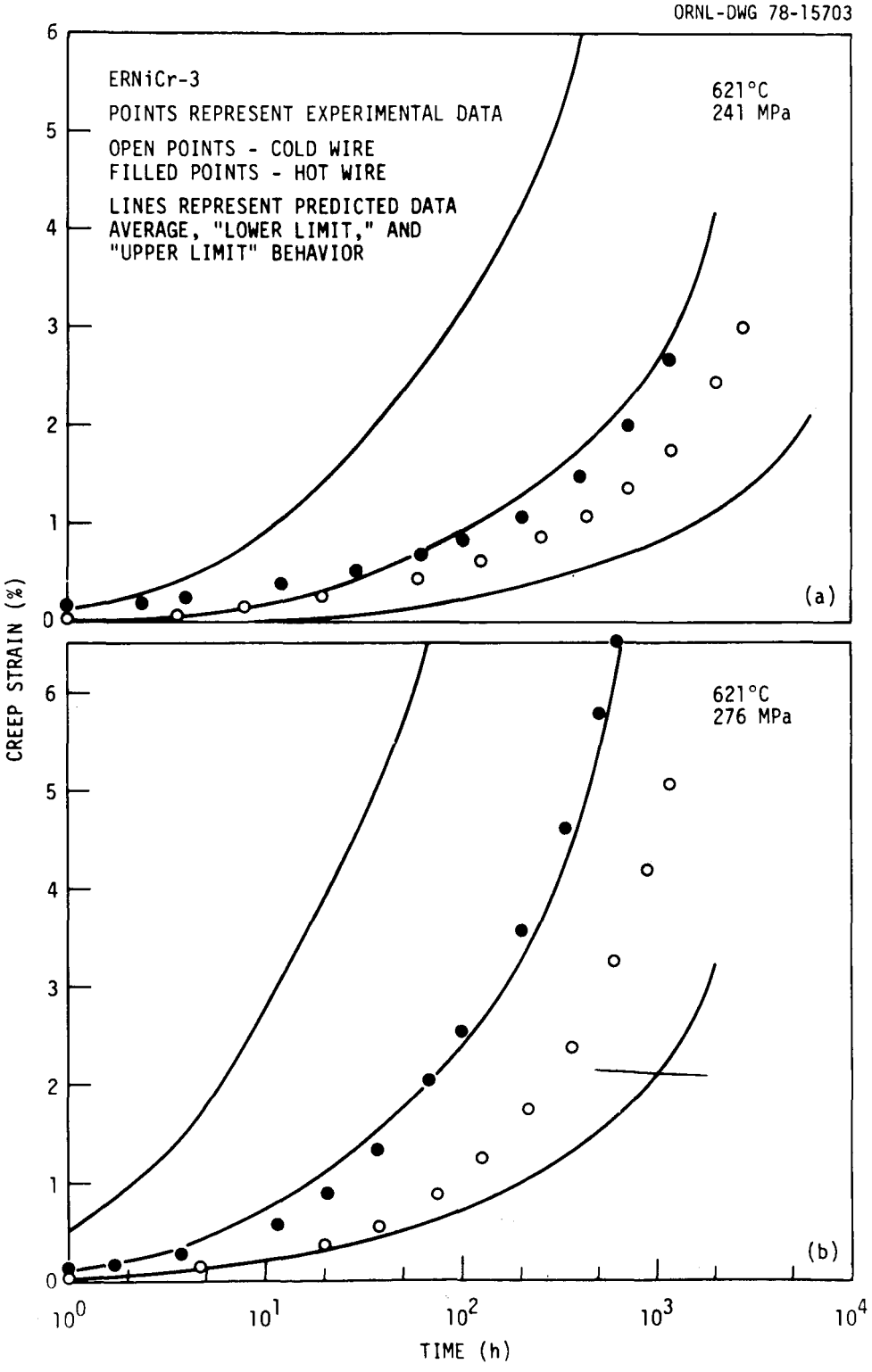

Fig. 27. Comparison of Predicted and Experimental Creep Behavior at 621°C.

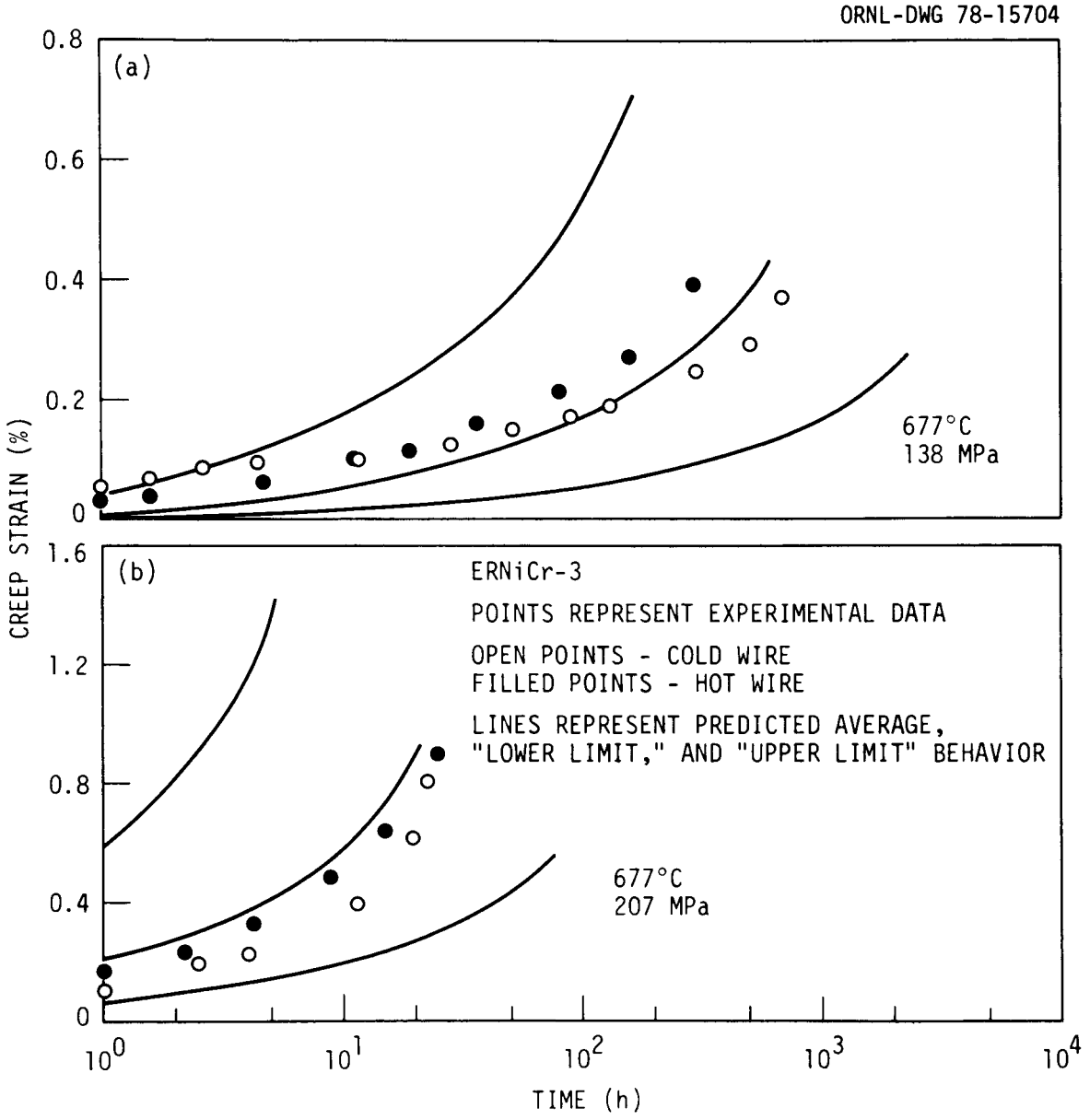

Fig. 28. Comparison of Predicted and Experimental Creep Behavior at 677°C.

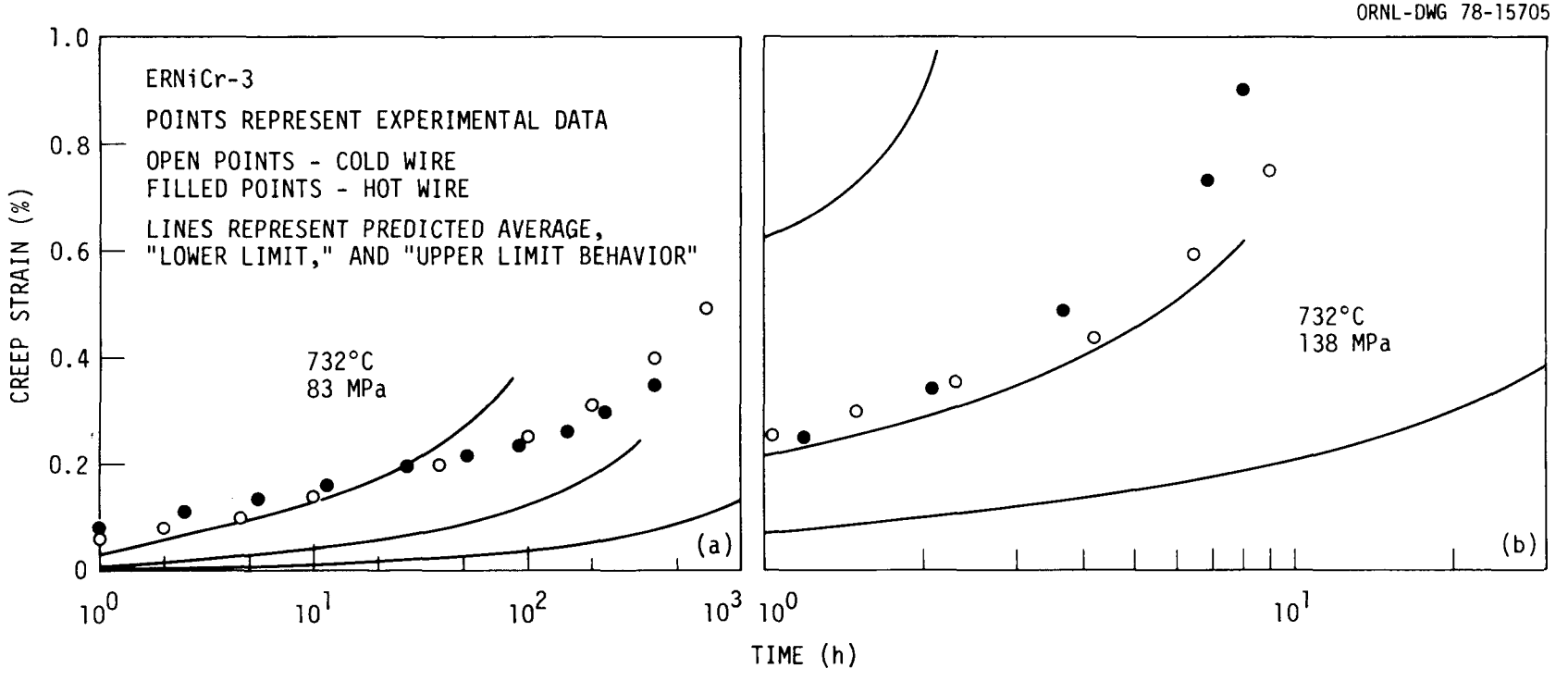

Fig. 29. Comparison of Predicted and Experimental Creep Behavior at 732°C.

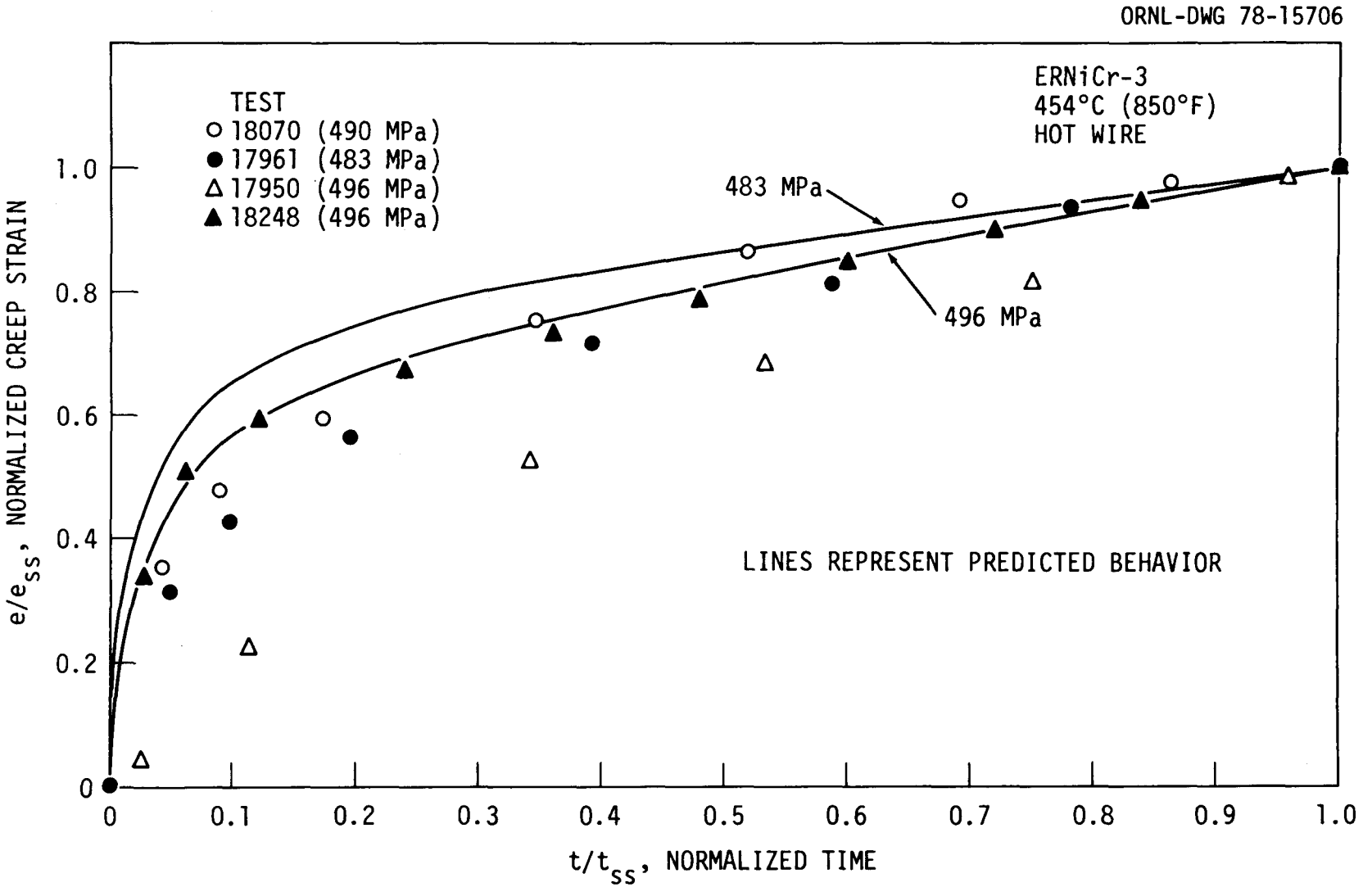

Fig. 30. Comparison Between Predicted and Experimental Normalized Creep Curves at 454°C.

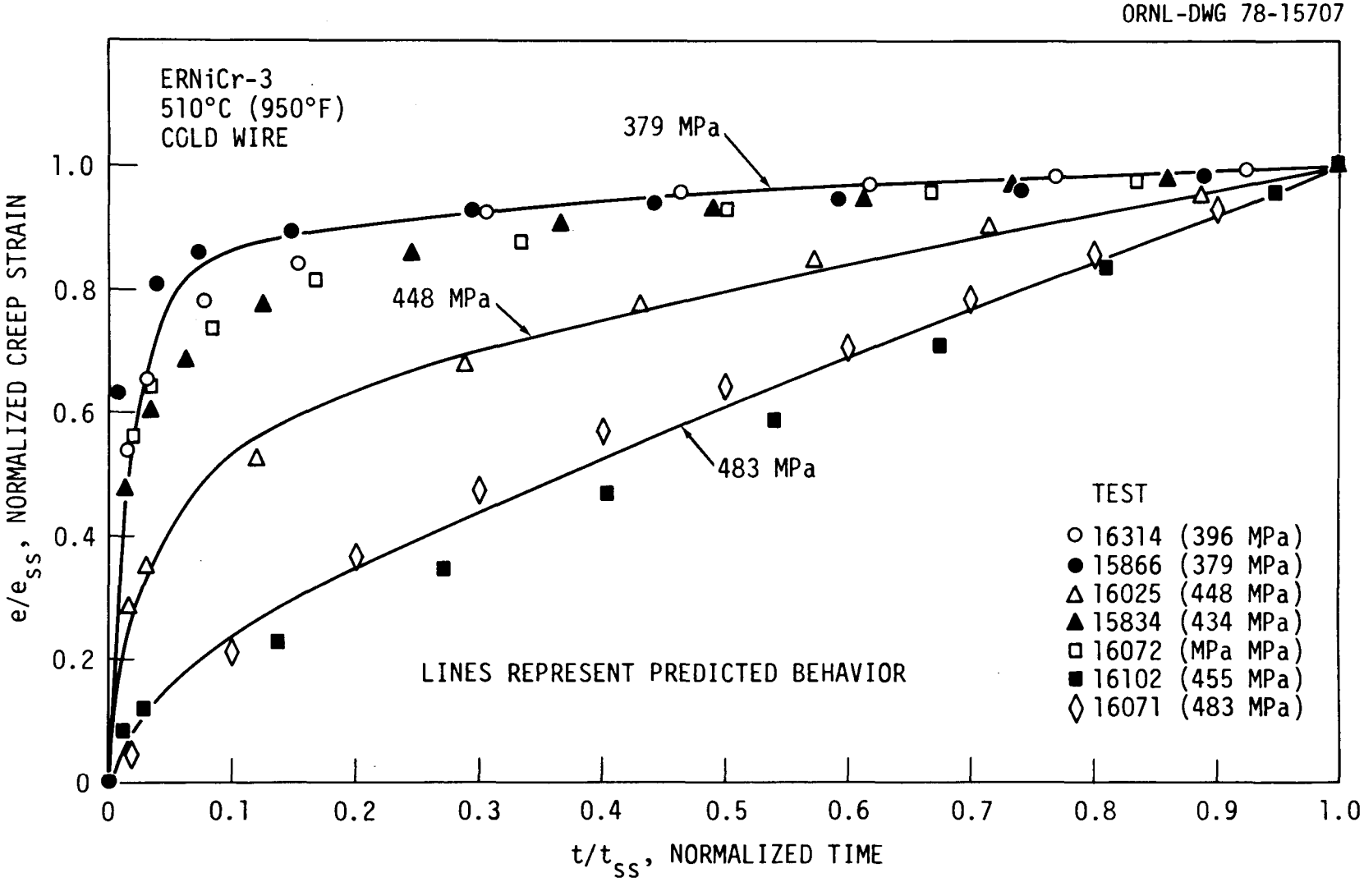

Fig. 31. Comparison Between Predicted and Experimental Normalized Creep Curves at 510°C.

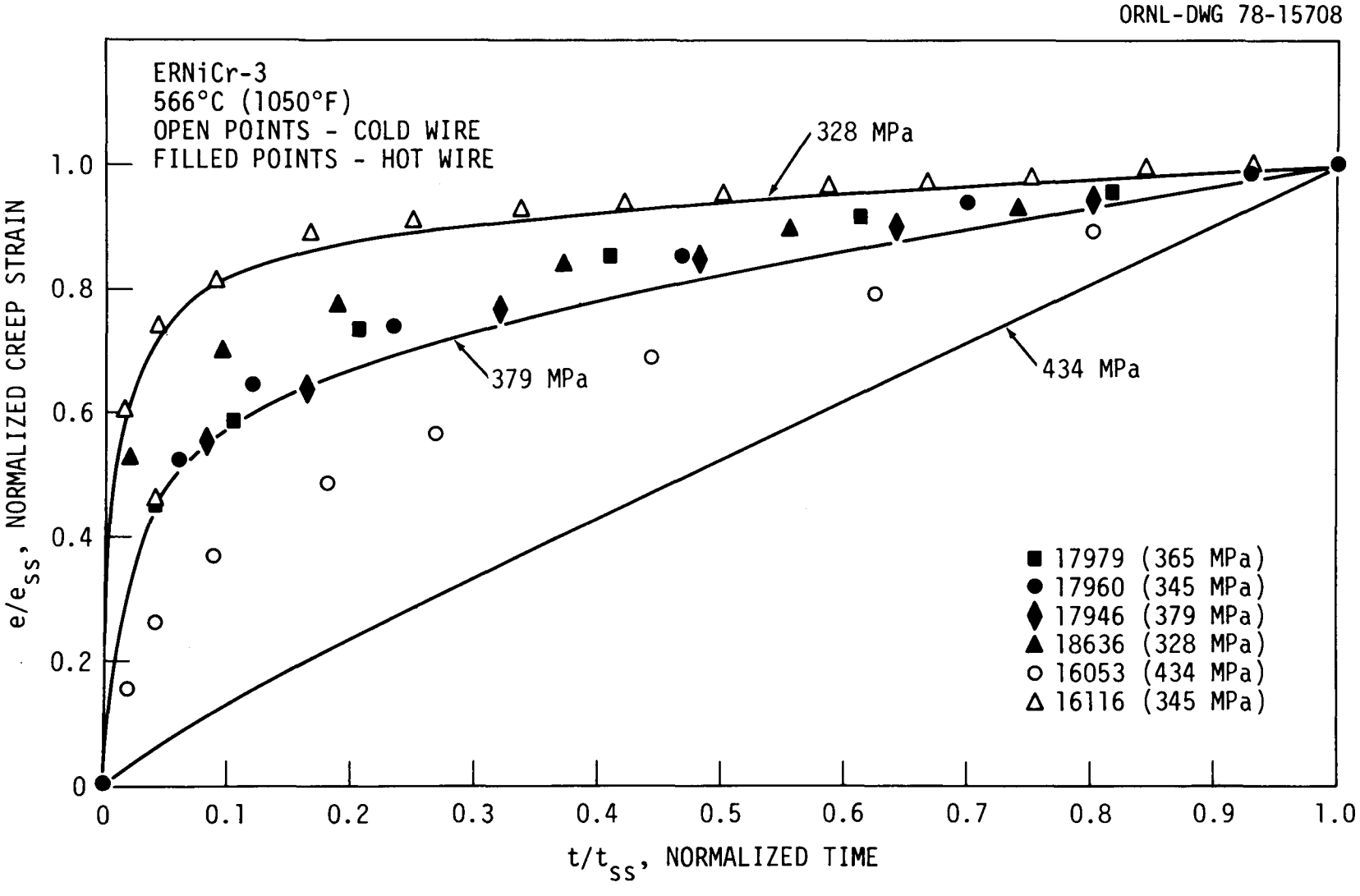

Fig. 32. Comparison Between Predicted and Experimental Normalized Creep Curves at 566°C.

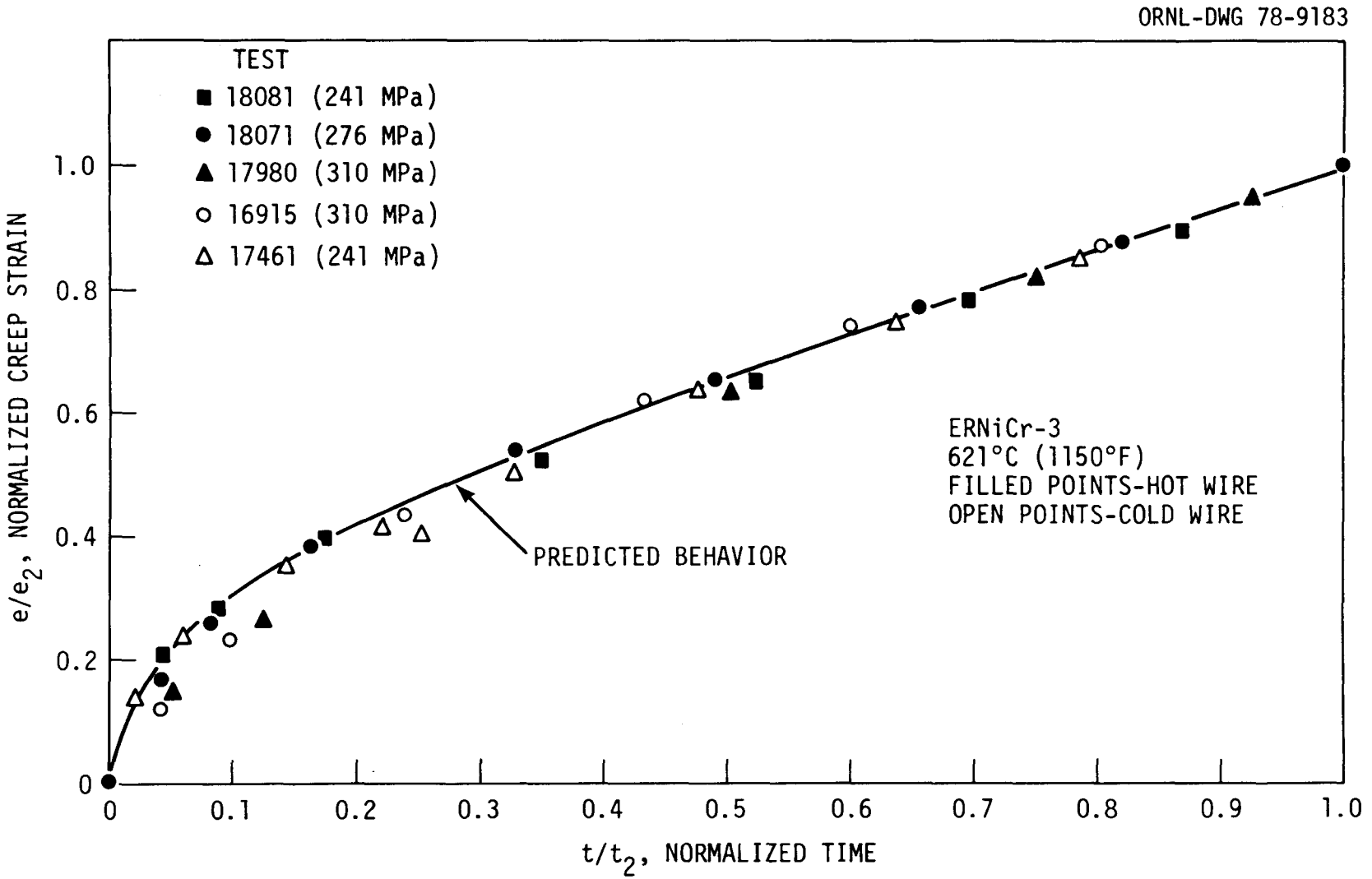

Fig. 33. Comparison Between Predicted and Experimental Normalized Creep Curves at 621°C.

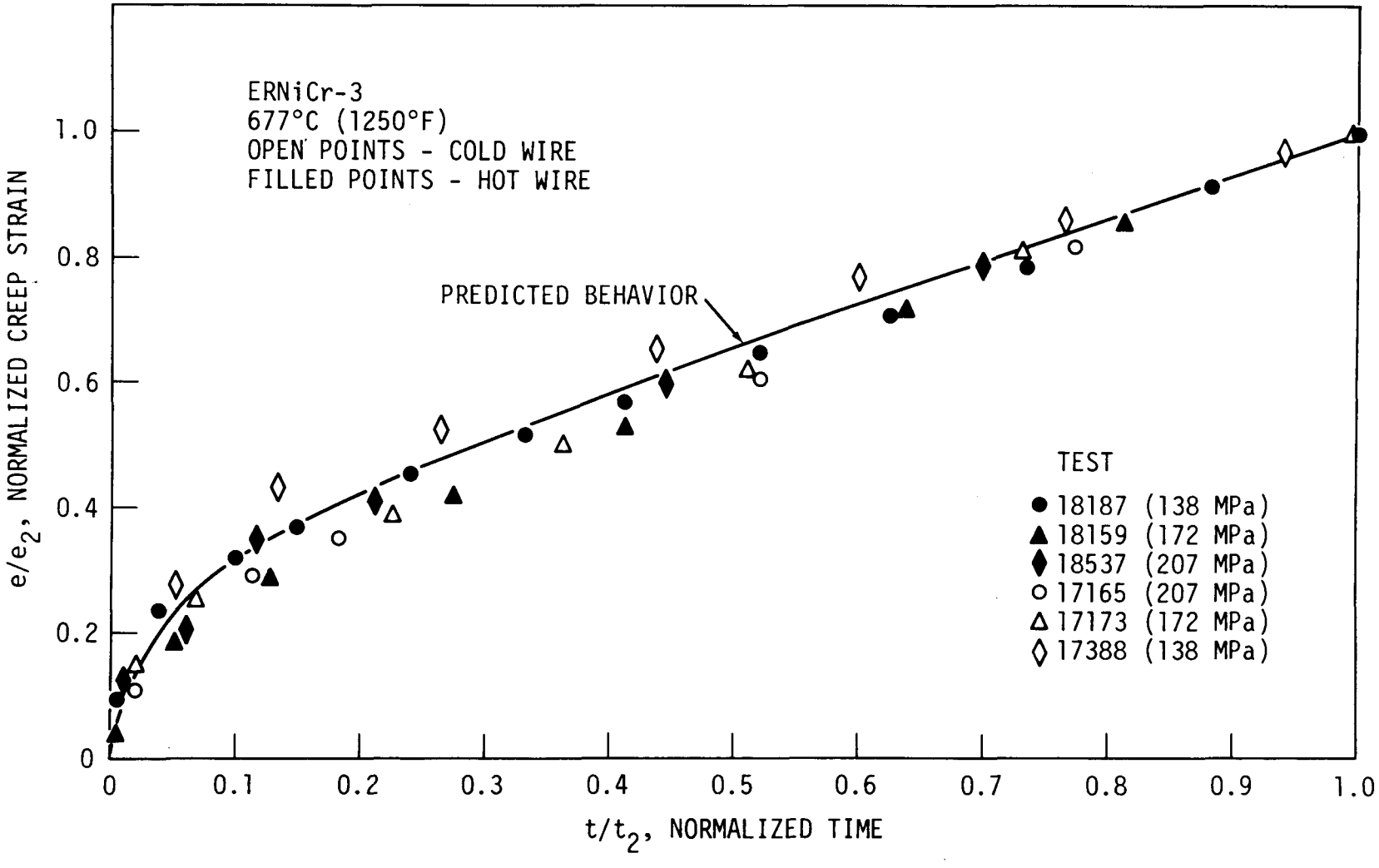

Fig. 34. Comparison Between Predicted and Experimental Normalized Creep Curves at 677°C.

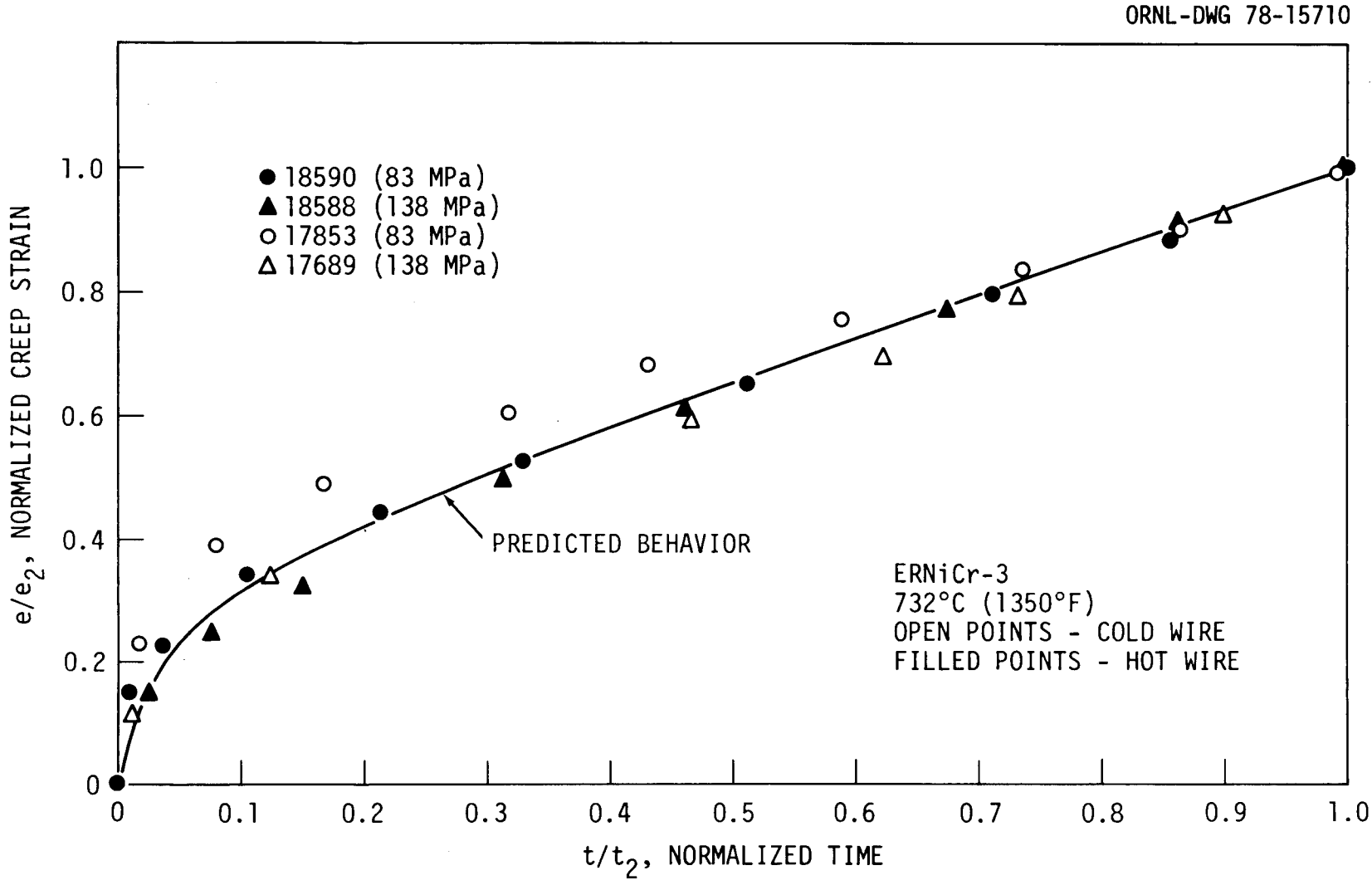

Fig. 35. Comparison Between Predicted and Experimental Normalized Creep Curves at 732°C.

calculated results is good. Note that the equations predict (and the data show) that all the high-temperature tests will fall on a single normalized "master creep curve."[13] This phenomenon occurs because the forms of Eqs. (8) and (21) dictate that p' and $\dot{e}_m'$ are constants in this region. The value of C' is also constant, since it depends only on p' and $\dot{e}_m'$. With all three normalized equation parameters being constant, normalized creep predictions at all stresses and temperatures in this region are identical. The forms of Eqs. (7) and (20) preclude the existence of a master creep curve in the low-temperature region. In that range, as t_{ss} becomes larger and $\dot{e}_m$ becomes smaller, the primary creep portion of the curve becomes sharper and more dominant relative to the secondary portion. This trend is most clearly seen at 510°C (Fig. 31).

Extrapolation of Results

The above analytical results provide a good description of trends in available creep and creep-rupture data for ERNiCr-3 weld metal. However, those data were obtained at stresses well above those that would generally be seen in an actual design situation. Therefore, the results must be extrapolated well beyond the range of available data before they can be of use in design calculations. As an example, CRBRP design[15] will require creep calculations for this material approximately in the range 454-593°C with most service[16] being at or below 566°C. At these temperatures 2 1/4 Cr-1 Mo steel is weaker than either ERNiCr-3 or alloy 800H. Therefore, the strength of this material would be expected to somewhat limit design stresses. ASME Code Case 1592 gives[17] the allowable stress intensity values for 2 1/4 Cr-1 Mo steel for a 3×10^5-hr design life as 85 MPa at 454°C, 50 MPa at 510°C, and 28 MPa at 566°C — all well below the range of available data for ERNiCr-3.

Extrapolations beyond the range of any data cannot be verified as accurate in the absence of a detailed physical theory for the processes involved. No such theory presently exists for the creep and creep-rupture of ERNiCr-3 weld metal. Any extrapolations could differ considerably from true behavior as a result of long-term metallurgical changes in the material involved or changes in the dominant deformation and/or

failure mechanisms.[11] Extrapolation of the current low-temperature results to design stress levels involves several uncertainties, even beyond the usual questions that occur in the extrapolation of creep data.

First, the analysis here has ignored the occurrence of the "strain burst" phenomenon. Whether this phenomenon would occur under design conditions could be an important design factor. Second, the available low-temperature data were all obtained at stresses that yield high plastic strains on loading (see Appendix). At design stresses such time-independent plastic strains would probably be negligible. There is no real information concerning the interaction between the plasticity and creep behavior of this material. Creep behavior in the absence of plastic strain might differ considerably from behavior in the presence of significant plastic strains. Finally, note that the log σ-log t_r and log σ-log $\dot{e}_m$ isotherms are extremely "flat" at the lower temperatures. Table 3 gives typical tensile data[18] for this material. The table shows that the creep stresses of the lower temperature data are approaching the ultimate tensile strength of the material. Since the stress cannot exceed this value, the isotherms are thus forced to be flat in this region. This flatness may simply be a manifestation of the approach of the stresses to the value of the ultimate tensile strength and not an indication of true material behavior. Klueh[5] has noted some tendency for these isotherms to break downward as stresses decrease, but the current analyses show that this break is not significant and that the data can be described by linear log-log isotherms. Still, as stresses become lower the curves may indeed break downward. Direct extrapolation of Eqs. (1) through (4) would in that case yield overoptimistic results.

One possible analytical approach to establishing the long-time stress dependence at the lower temperatures is to extrapolate the results from the high-temperature data downward in temperature, since the high-temperature data were obtained at stresses well below the ultimate. Figure 36 illustrates results obtained by extrapolating Eq. (4) downward in temperature and matching those predictions with the predictions of Eq. (2). The results look reasonable, but there is no real reason to expect that the same mechanisms will be active over the entire range of

Table 3. Tensile Properties of ERNiCr-3 Weld Metal[a] at a Strain Rate[b] of 3.0×10^{-4}/s

Test Temperature (°C)	Test Temperature (°F)	Strength, MPa (ksi) Yield	Ultimate	Fracture	Elongation, % Uniform	Total	Reduction of Area (%)
			Plate 1				
25	77	295(42.9)	610(88.6)	483(70.1)	39.1	43.9	45.8
25	77	311(45.2)	622(90.3)	474(68.8)	33.3	37.6	44.4
454	850	219(31.8)	507(73.6)	442(64.1)	41.8	46.8	47.7
510	950	229(33.3)	488(70.8)	413(59.9)	35.8	38.9	40.0
566	1050	220(32.0)	478(69.4)	377(54.6)	39.2	43.0	51.6
621	1150	203(29.5)	421(61.3)	237(34.2)	32.8	38.0	47.0
			Plate 2				
25	77	335(51.3)	658(95.5)	476(69.1)	30.4	34.7	44.1
204	400	305(44.3)	575(83.4)	473(68.7)	34.3	36.7	45.6
316	600	298(43.2)	548(79.6)	452(65.6)	26.4	29.9	45.5
454	850	282(41.0)	542(78.7)	474(68.9)	36.8	40.6	43.7
510	950	267(38.8)	501(72.7)	369(53.5)	33.9	37.1	40.1
566	1050	259(37.6)	486(70.6)	371(53.9)	33.6	37.6	51.5
621	1150	258(37.4)	451(65.4)	265(38.4)	25.8	29.4	50.4
677	1250	256(37.1)	405(58.8)	62(9.0)[c]	15.3	19.0[c]	30.9[c]
677	1250	247(35.8)	422(61.2)	141(20.4)	19.9	28.3	46.9
732	1350	261(37.9)	327(47.2)	124(18.0)	4.1	29.9	53.7
			Plate 3				
25	77	339(49.2)	601(87.3)	476(69.1)	32.8	39.3	43.6
204	400	292(42.4)	557(80.8)	421(61.1)	35.1	40.2	47.0
316	600	264(38.3)	524(76.0)	355(51.5)	33.8	38.1	46.9
454	850	274(39.7)	490(71.1)	416(60.3)	32.7	36.3	45.8
510	950	258(37.4)	477(69.2)	388(56.3)	30.1	33.2	39.7
566	1050	240(34.8)	451(65.4)	347(50.4)	33.0	35.3	37.4
621	1150	251(36.5)	444(64.4)	101(14.7)	31.6	36.6	46.7
677	1250	236(34.3)	413(60.0)	130(18.8)	23.0	31.8	51.4
732	1350	228(33.1)	335(48.6)	85(12.3)	7.7	41.7	68.5
			Plate 4				
25	77	351(51.0)	618(89.7)	471(68.3)	36.2	40.7	59.1
204	400	262(38.0)	557(80.9)	449(65.1)	40.7	44.9	50.5
316	600	260(37.7)	535(77.6)	428(62.1)	36.6	40.5	49.8
454	850	249(36.2)	515(74.7)	431(62.6)	41.6	46.6	50.7
510	950	243(35.3)	493(71.6)	436(63.3)	40.4	44.6	57.2
566	1050	256(37.2)	465(67.5)	373(54.1)	33.7	37.1	51.6
621	1150	267(38.8)	449(65.2)	359(52.1)	28.6	32.7	49.0
677	1250	251(36.5)	422(61.2)	155(22.5)	22.2	33.6	55.6
732	1350	262(38.0)	338(49.0)	55(8.0)	6.7	39.8	42.2

[a]All specimens were postweld heat-treated for 1 hr at 732°C (1350°F).

[b]Tests were at a constant crosshead speed of 8.5 μm/s.

[c]Failed near end of gage section at point where extensometer was attached.

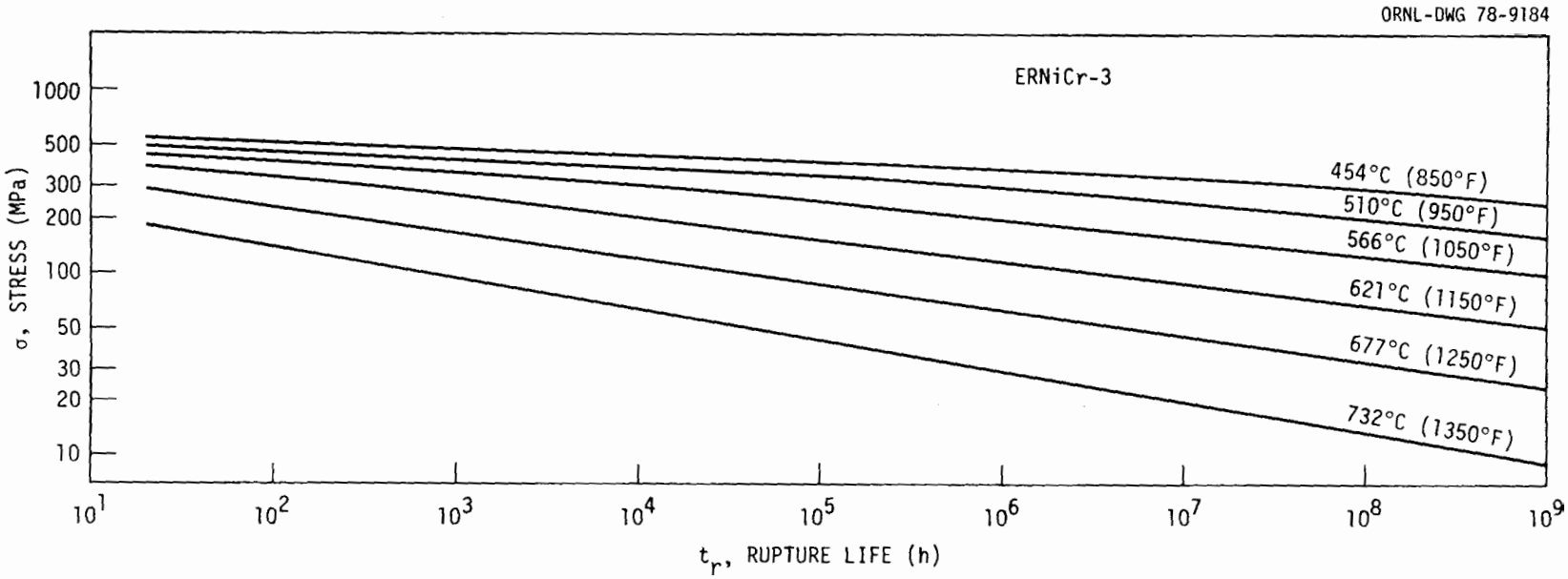

Fig. 36. Predicted Stress-Rupture Isotherms for ERNiCr-3 Weld Metal, Including Prediction of Long-Term Behavior.

temperatures. Also, even if the low-temperature stress dependence can be described by Eqs. (3) and (4), temperature-dependent effects (e.g., recovery) might make the tertiary creep and creep strain-time behavior different in the two temperature regions. Three analytical possibilities thus present themselves from the available information: (1) extrapolate the low-temperature analysis directly; (2) extrapolate the high-temperature analysis to low temperatures directly; and (3) extrapolate $\dot{e}_m$ and t_r from the high-temperature analysis and t_3, e_3, C, and p from the low-temperature analysis. However, a modification must be made in order to obtain consistent results from this third approach. The ratio $\dot{e}_m/t_r$ is much higher from Eqs. (3) and (4) than from Eqs. (1) and (2). As a result, using Eqs. (3) and (4) in conjunction with low-temperature equations relating t_3 and t_r and $\dot{e}_3$ and $\dot{e}_m$ yields unreasonably high values for e_3. In the low-temperature region, $\dot{e}_m$ and t_r can be related by

$$\dot{e}_m = 31 t_r^{-1.56} \quad . \tag{22}$$

Extrapolation method 3 above can thus be effected by use of Eq. (4) to yield $t_r(\sigma,T)$, use of Eq. (22) to yield $\dot{e}_m$, and use of the low-temperature equations to yield e_3, C, and p from these values. Table 4 summarizes typical predictions made from these three approaches for reasonable design stress-temperature conditions. In all cases very little creep strain is predicted within a 3×10^5-hr design life. However, the predictions do vary very widely, with method 1 being the most conservative and method 3 being the least.

The available data do not allow an assessment as to which of the three extrapolation methods is most accurate. An ongoing single test at 241 MPa (35.0 ksi) and 454°C has shown essentially no creep in 1000 hr, which is consistent with all three prediction methods. All methods underestimate the amount of creep occurring in 1000 hr in the tests of Swindeman[19] at 538 and 593°C from 103 to 172 MPa, with method 3 coming closest. However, these tests are of too short duration compared with the total life under these stress-temperature conditions to make any meaningful comparisons about the magnitude of the predicted strain.

Table 4. Predicted Creep Behavior of ERNiCr-3 Under Estimated Typical CRBRP Transition Joint Normal Operating Stresses

Prediction Method[a]	Predicted Values of: t_r (hr)	$\dot{e}_m$ (%/hr)	t_3 (hr)	e_3 (%)	e(% in 3×10^5 hr)
			454°C (850°F), 80 MPa		
1	7.8×10^{23}	2.6×10^{-41}	7.6×10^{23}	2.3×10^{-7}	1.5×10^{-17}
2	3.1×10^{15}	2.6×10^{-19}	1.9×10^{15}	7.2×10^{-4}	1.1×10^{-12}
3	3.1×10^{15}	2.1×10^{-23}	3.1×10^{15}	2.5×10^{-2}	1.0×10^{-6}
			510°C (950°F), 45 MPa		
1	3.7×10^{24}	4.5×10^{-42}	3.7×10^{24}	3.0×10^{-7}	6.6×10^{-18}
2	1.6×10^{15}	4.9×10^{-19}	9.8×10^{14}	7.3×10^{-4}	2.2×10^{-12}
3	1.6×10^{15}	5.7×10^{-23}	1.6×10^{15}	2.8×10^{-1}	1.8×10^{-6}
			566°C (1050°F), 25 MPa		
1	8.7×10^{23}	2.4×10^{-40}	8.5×10^{23}	1.4×10^{-6}	8.2×10^{-17}
2	3.8×10^{14}	1.6×10^{-18}	2.3×10^{14}	5.5×10^{-4}	6.9×10^{-12}
3	3.8×10^{14}	5.6×10^{-22}	3.7×10^{14}	3.6×10^{-1}	6.2×10^{-6}

[a]Method 1 involves direct extrapolation of low-temperature analysis; Method 2 involves direct extrapolation of high-temperature analysis; Method 3 involves extrapolation of high-temperature equations for t_r, then uses those values in the low-temperature equations to make other predictions.

Significantly, these tests do exhibit most of their creep in a short rapid initial transient — a behavior qualitatively consistent with the low-temperature curve shapes as depicted in either method 1 or method 3.

Swindeman[19] also ran two relaxation tests on ERNiCr-3, one each at 538 and 593°C after 30 strain cycles at a total strain range of 0.4%. There is no real information concerning the effect of strain cycling on creep or relaxation of this material, so the above three prediction methods were used directly in conjunction with the hypothesis of strain hardening (recommended for use with 2 1/4 Cr-1 Mo steel[20]) in an attempt to model the relaxation behavior of this material. The stress levels in these tests are all well below the range of available creep data from the current study, so this comparison provides some check of the extrapolation techniques. As shown in Fig. 37, method 3 appears to provide the best predictions for these data.

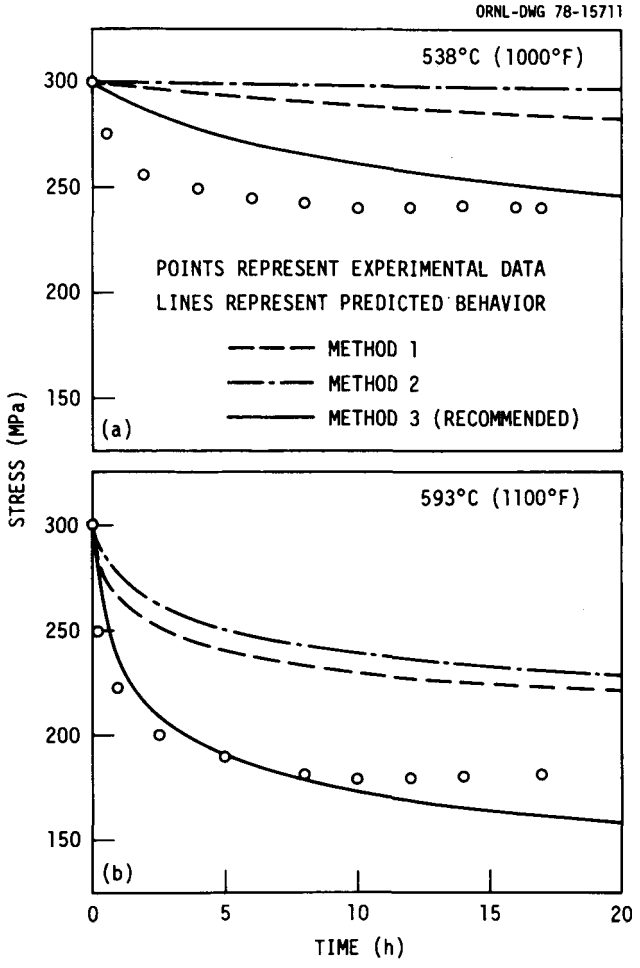

Fig. 37. Comparison of Predicted Experimental Relaxation Data for ERNiCr-3 Weld Metal with Behavior Predicted by Several Methods.

On the basis of all the above considerations (which are still not very conclusive), method 3 was selected as the best extrapolation scheme at this time. This choice cannot be verified by available data. However, as can be seen from Table 4, under most operating conditions for the proposed CRBRP transition joint, ERNiCr-3 is sufficiently stronger than 2 1/4 Cr-1 Mo that it will exhibit essentially no creep. Upset and transient conditions may, however, cause more severe stress-temperature conditions under which ERNiCr-3 may undergo creep deformation and/or stress relaxation. Moreover, stress redistributions may cause the stress in the weld metal to significantly exceed that in the 2 1/4 Cr-1 Mo base metal.[21]

DISCUSSION

The general techniques used for the analysis of the current data have been described extensively elsewhere[1-4,7-14] and will not in themselves be discussed in detail here. It should be pointed out, however, that Eqs. (5) through (8), (20), and (21) may be oversimplifications of real behavior. Still, the current data do not warrant more complicated analysis. Uncertainties will remain in any case, and the current simple approaches, while yielding some inconsistencies with the data (e.g., the general overprediction of creep strain at 454°C), do a good job of capturing the general trends in the data.

The effect of minor inconsistencies and simplifications on the results must be viewed within the framework of the scatter and uncertainty inherent in the data. Several tests were run under nominally identical conditions, and these duplicate tests can be used to obtain an estimate of the amount of scatter inherent in the data. A straightforward examination of the data in the Appendix reveals that t_r may easily vary by a factor of 100 or more simply from scatter in the data. Other quantities used in the analysis, such as t_3 and $\dot{e}_3$, display similar amounts of scatter. In view of this large variation in the data themselves, some simplification in the analysis can be justified. For example, at long times and high temperatures (677-732°C) t_2 was somewhat arbitrarily set at $0.6t_r$. From the above discussion the value may actually be anywhere from $0.2t_r$ to t_r. This uncertainty of a factor of three or less appears quite acceptable in view of the total scatter in the data.

Design applications will require use of predictions well outside the range of experimental data, however. As mentioned above, the current data for ERNiCr-3 present some difficult extrapolation problems, especially at the lower temperatures (454-566°C), where available data may give no true indication of the long-term stress dependence of the creep response. The extrapolation method selected for these data (method 3 above) uses high-temperature (621-732°C) data to predict the stress dependence of creep at low temperatures but uses low-temperature data to predict the shapes of the creep strain-time curves. This approach is felt to be the best choice based on available information, but more information is

needed to verify its accuracy. Prediction of low-temperature stress dependence based on higher temperature data is a common practice in the analysis of creep data, but it nonetheless may be inaccurate if different mechanisms operate at the different temperatures. More low-stress creep data and creep relaxation data would be extremely useful in adding confidence to the extrapolations. Data on effects of cyclic loading and of variable stresses and temperatures would also be valuable.

Another potentially important concern for design is the strain burst phenomenon noted above. That phenomenon has been ignored in the current analysis and thus will not be reflected in any of the current predictions. Klueh[5,6] has postulated that the effect may be due to the sudden release of dislocation pileups caused by regions of short-range order in the alloy or by inhomogeneities in the weld metal microstructure. Another possibility is that the bursts are some form of time-delayed plasticity caused mainly by the extremely high stresses involved. At any rate, design stress conditions would certainly preclude the occurrence of such a plasticity effect under design operating conditions. Moreover, since the alloy would generally be expected to experience negligible amounts of plastic deformation, it may also be difficult to build up concentrated dislocation pileups such as might cause the strain bursts per Klueh's[5,6] explanation. Therefore, it might be argued — but not proved — that the strain bursts will not occur under design conditions, and therefore can indeed safely be ignored.

Finally, Fig. 38 compares the predicted creep rupture strength of ERNiCr-3 from 454 to 566°C with those of alloy 800H and 2 1/4 Cr-1 Mo steel, the two alloys it would join in the proposed CRBRP transition joint. The creep strengths would compare similarly. As can be seen from the figure, the ferritic 2 1/4 Cr-1 Mo steel is significantly weaker than the other two alloys. The horizontal line for the alloy 800H represents the predicted[3] ultimate tensile strength at each temperature. For that alloy, data at 538°C and above were extrapolated downward in temperature to yield the predictions shown in the figure. For times at which the predicted rupture strength was greater than the ultimate tensile strength, the value has simply been replaced by the tensile strength value, thus the horizontal lines. Thus, the low-temperature

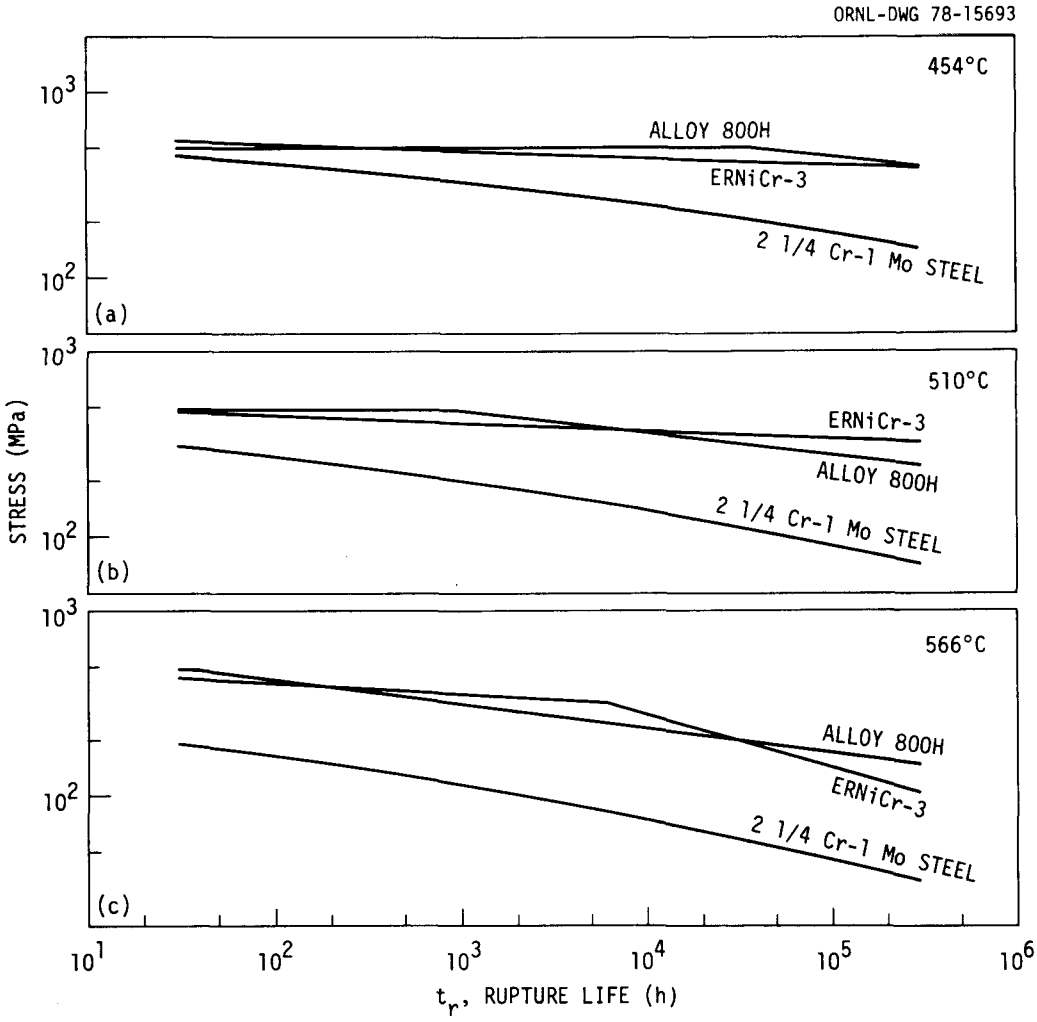

Fig. 38. Comparison of Predicted Stress-Rupture Behavior for ERNiCr-3 Weld Metal, Alloy 800H, and 2 1/4 Cr-1 Mo Steel at (a) 454°C, (b) 510°C, and (c) 566°C.

creep behavior of alloy 800H would also be different from what would be predicted by the higher temperature data. This fact reinforces the view that the difference in the stress dependence of ERNiCr-3 at low and high temperatures is caused largely by the fact that the creep stresses at low temperatures are near the tensile strength, forcing flatness in the log σ-log t_r and log σ-log $\dot{e}_m$ isotherms. It also lends support to the extrapolation method used herein to predict the long-time stress dependence at low temperatures.

SUMMARY

Creep and creep-rupture data for ERNiCr-3 appear to show different behavior in the range 454 to 566°C than in the range 621 to 732°C. The average rupture life (t_r) and minimum creep rate ($\dot{e}_m$) can be related to stress (σ, MPa) and temperature (T, K) in these two regions by Eqs. (1) through (4) in the text, although the data exhibit considerable scatter. In the range 454 to 621°C the time to tertiary creep, t_3, was predicted by

$$t_3 = 0.98t_r \ , \tag{5}$$

while in the range 677 to 732°C the relationship was

$$t_3 = 0.028t_r^{1.2} \ , \tag{6}$$

or

$$t_3 = 0.6t_r \ , \tag{23}$$

whichever yields a smaller value.

Defining the average creep rate to tertiary creep as $\dot{e}_3 = e_3/t_3$, where e_3 is the strain to tertiary creep, we found in the range 454 to 566°C

$$\dot{e}_3 = 0.84\dot{e}_m^{0.75} \tag{7}$$

and in the range 621 to 732°C

$$\dot{e}_3 = 1.5\dot{e}_m \ . \tag{8}$$

The strain to tertiary creep can then be predicted from $e_3 = \dot{e}_3 t_3$ at all temperatures.

The creep strain-time behavior was described at all temperatures by the rational polynomial creep equation,

$$e = \frac{Cpt}{1 + pt} + \dot{e}_m t \ , \tag{12}$$

where

e = creep strain

t = time

$\dot{e}_m$ = minimum creep rate, and

C = the limiting value of the transient primary creep strain.

The parameter p is related to the sharpness of the curvature of the primary creep region.

In the range 454 to 566°C p was given by

$$p = 6.5 t_3^{-0.69} \ , \tag{20}$$

while in the range 621 to 732°C, the relationship was

$$p = 26/t_3 \ . \tag{21}$$

At all temperatures C is given by

$$C = e_3 \left(\frac{1 + pt_3}{pt} \right) (1 - \dot{e}_m/\dot{e}_3) \ . \tag{24}$$

Extrapolation of the current analyses to long-term behavior involves large uncertainties and should be done with caution. The high-temperature results can be extended directly for $T > 593$°C. The higher creep stresses at the low temperatures ($T \leqslant 593$°C) are all very near the ultimate tensile strengths at those temperatures. Thus, log σ-log t_r isotherms are forced to be flat and do not reflect the true stress dependence. At

long times the high-temperature data were extrapolated downward in temperature to estimate the stress dependence. Thus, t_r is predicted from Eq. (2) or (4), whichever yields the smaller value. If Eq. (4) is used, $\dot{e}_m$ should be predicted from

$$\dot{e}_m = 31 t_r^{-1.56} , \tag{22}$$

to yield consistent results. Other low-temperature equations remain unchanged. The net effect is to predict the stress dependence from the high-temperature data but to predict the creep curve shapes from the low-temperature data. These predictions compare reasonably well with available low-stress creep and relaxation data. However, it must be realized that this extrapolation scheme is based on assumptions that cannot be verified by the current data. The low-temperature predictions can be made as low as 427°C (800°F), but once again one must be careful of estimating creep stresses above the tensile strength at short times. All these analyses ignore the strain burst phenomenon that has been observed[5,6] in this alloy, but there is some reason to believe that these bursts may not occur under CRBRP design conditions. All results should be considered interim; more data are needed to verify the accuracy of the results.

ACKNOWLEDGMENTS

The authors would like to thank J. F. King for supplying the welds tested in this evaluation. Thanks also go to D. O. Hobson and W. K. Sartory for reviewing the manuscript and to S. Peterson for editing and Ethel Cagle for preparing the final report.

REFERENCES

1. M. K. Booker, *Interim Analysis of the Creep Strain-Time Characteristics of Annealed and Isothermally Annealed 2 1/4 Cr-1 Mo Steel*, ORNL/TM-5831 (June 1977).
2. M. K. Booker, "Analytical Description of the Effects of Melting Practice and Heat Treatment on the Creep Properties of 2 1/4 Cr-1 Mo Steel," pp. 323-43 in *Effects of Melting and Processing Variables on the Mechanical Properties of Steel*, MPC-6, G. V. Smith, ed., American Society of Mechanical Engineers, New York, 1977.
3. M. K. Booker, V. B. Baylor, and B. L. P. Booker, *Survey of Available Creep and Tensile Data for Alloy 800H*, ORNL/TM-6029, (January 1978).
4. M. K. Booker, "An Analytical Representation of the Creep and Creep-Rupture Behavior of Alloy 800H," pp. 1-28 in *Characterization of Materials for Elevated Temperature Service*, American Society of Mechanical Engineers, New York, 1978.
5. R. L. Klueh and J. F. King, *Creep and Creep-Rupture Behavior of ERNiCr-3 Weld Metal*, ORNL-5404, June 1978.
6. R. L. Klueh and J. F. King, *Mechanical Properties of ERNiCr-3 Weld Metal Deposited by Gas-Tungsten-Ore Process with Hot Wire Filler Additions*, ORNL-5491.
7. M. K. Booker, "Use of Generalized Regression Models for the Analysis of Stress-Rupture Data," pp. 459-500 in *Characterization of Materials for Elevated Temperature Service*, American Society of Mechanical Engineers, New York, 1978.
8. M. K. Booker and V. K. Sikka, "Interrelationships Between Creep Life Criteria for Four Nuclear Structural Materials," *Nucl. Technol.* 30: 52-64 (July 1976).
9. M. K. Booker and V. K. Sikka, *Empirical Relationships Among Creep Properties of Four Elevated-Temperature Structural Materials*, ORNL/TM-5399 (June 1976).
10. M. K. Booker and V. K. Sikka, *Predicting the Strain to Tertiary Creep for Elevated-Temperature Structural Materials*, ORNL/TM-5403 (July 1976).
11. M. K. Booker, *Mathematical Analysis of the Elevated-Temperature Creep Behavior of Type 304 Stainless Steel*, ORNL/TM-6110 (December 1977).

12. M. K. Booker and V. K. Sikka, *Analysis of the Creep Strain-Time Behavior of Type 304 Stainless Steel*, ORNL-5190 (October 1976).
13. M. K. Booker, *An Interim Analytical Representation of the Creep Strain-Time Behavior of Commercially Heat-Treated Alloy 718*, ORNL/TM-6232, May 1978.
14. D. O. Hobson and M. K. Booker, *Materials Applications and Mathematical Properties of the Rational Polynomial Creep Equation*, ORNL-5202 (December 1976).
15. LMFBR Demonstration Plant Development Requirements Specification, Development Task No. 51.39 — "Transition Joint Development Support," 1976.
16. A. W. Dalcher, General Electric Company, private communication, 1978.
17. *Interpretations of the ASME Boiler and Pressure Vessel Code, Case 1592*, American Society of Mechanical Engineers, New York, 1974.
18. R. L. Klueh and J. F. King, *Elevated-Temperature Tensile Properties of ERNiCr-3 Weld Metal*, ORNL-5354 (December 1977).
19. R. W. Swindeman, ORNL, private communication, 1977.
20. C. E. Pugh et al., *Background Information for Interim Methods of Inelastic Analysis for High-Temperature Reactor Components of 2 1/4 Cr-1 Mo Steel*, ORNL/TM-5226 (May 1976).
21. T. J. Delph, ORNL, private communication, 1978.

APPENDIX

DATA USED IN ANALYSES

Data Used in Analyses

Temperature (°C)	Stress (MPa)	Rupture Life (h)	Time to Tertiary Creep[a] (h)	Strain to Tertiary Creep[b] (%)	Minimum Creep Rate (%/h)
		Hot Wire			
454	483	512	510	3.20	0.0018
454	490	1158	1157	3.70	0.00086
454	496	44	37	1.66	0.035
454	496	1671	1670	3.55	0.00069
510	396	6638	6635	0.95	0.000075
510	414	1050	1049	3.00	0.00038
510	434	260	255	4.00	0.00353
510	448	106	90	4.20	0.016
566	328	2776	2700	2.85	0.00022
566	345	432	430	2.50	0.00116
566	365	247	244	3.40	0.00369
566	379	130	125	4.85	0.0092
621	241	1401	1150	2.68	0.00163
621	276	653	560	6.00	0.0073
621	310	205	180	7.55	0.0315
677	138	2263	300	0.40	0.000928
677	172	367	30	1.00	0.0256
677	207	183	20	0.80	0.0325
732	83	1527	400	0.25	0.000433
732	103	459	60	0.40	0.00321
732	138	77	8	0.90	0.0778
		Cold Wire			
454	483	75	74	2.70	0.0205
454	483	68	67	1.75	0.00735
454	490	1075	1070	1.80	0.00112
454	496	1013	1000	2.00	0.0007
454	510	142	141	3.70	0.0123
510	379	6770	6750	2.67	0.000043
510	396	3255	3250	1.60	0.000037
510	414	1645	1635	5.66	0.00048
510	434	1205	1200	4.10	0.00054
510	448	357	350	4.44	0.0044
510	455	39	37	5.62	0.14
510	465	37	36	8.10	0.18
510	483	11	10	6.20	0.45
566	345	6003	5995	2.00	0.000062
566	345	779	770	3.55	0.00045
566	365	1088	1070	4.55	0.00072
566	379	841	835	5.72	0.00098

Data Used in Analyses (continued)

Temperature (°C)	Stress (MPa)	Rupture Life (h)	Time to Tertiary Creep[a] (h)	Strain to Tertiary Creep[b] (%)	Minimum Creep Rate (%/h)
		Cold Wire (continued)			
566	396	448	445	6.25	0.0030
566	396	125	121	11.00	0.066
566	396	64	63	9.82	0.133
566	414	113	110	9.30	0.036
566	434	30	28	10.65	0.22
621	241	3109	2750	3.00	0.00082
621	276	1196	1020	4.40	0.00331
621	293	653	550	7.45	0.0098
621	310	295	240	9.6	0.025
621	379	21	8	5.63	0.64
677	138	3590	690	0.40	0.000312
677	172	778	55	0.80	0.00436
677	207	215	22	0.80	0.022
677	241	89	8	1.5	0.08
677	276	26	2	1.4	0.326
732	83	2793	700	0.50	0.000352
732	103	634	63	0.60	0.0038
732	138	104	9	0.80	0.0603
732	172	31	2	0.95	0.342

[a]Values in the temperature range 454-566°C represent t_{ss}, the 0.2% offset time to tertiary creep. Values in the range 621-732°C represent t_2, the time to first deviation from linear secondary creep.

[b]Determined after graphical "removal" of strain bursts where they existed.

Blank Page

ORNL/TM-6464
Distribution
Category
UC-79b, -h, -k

INTERNAL DISTRIBUTION

1-3. Central Research Library
4. Document Reference Section
5-14. Laboratory Records Department
15. Laboratory Records, ORNL RC
16. ORNL Patent Office
17-21. M. K. Booker
22-26. D. R. Distefano
27-29. M. R. Hill
30. J. F. King
31-33. R. T. King
34. J. M. Leitnaker
35. J. W. McEnerney
36. V. K. Sikka
37. J. H. Smith
38. J. O. Stiegler
39. T. Weerasooriya
40. C. L. White
41. R. W. Balluffi (consultant)
42. P. M. Brister (consultant)
43. W. R. Hibbard, Jr. (consultant)
44. N. E. Promisel (consultant)
45. J. T. Stringer
46. M. L. Mayfield

EXTERNAL DISTRIBUTION

47-48. DOE DIVISION OF REACTOR RESEARCH AND DEVELOPMENT, Washington, DC 20545

Director

49. DOE OAK RIDGE OPERATIONS OFFICE, P.O. Box E, Oak Ridge, TN 37830

Assistant Manager, Energy Research and Development

50-312. DOE TECHNICAL INFORMATION CENTER, Office of Information Services, P.O. Box 62, Oak Ridge, TN 37830

For distribution as shown in TID-4500 Distribution Category, UC-79b (Fuels and Materials Engineering Development); UC-79h (Structural Materials Design Engineering); UC-79k (Components)